AN ABSTRACT OF THE THESIS OF

Rui Liu for the degree of Master of Science in Electrical and Computer Engineering presented on June 7, 2017.

Title: High Torque Density Cycloid Electrical Machine for Robotic Application

Abstract approved:

Julia Zhang

This thesis investigates a novel cycloid electric machine that integrates both cycloid gear drive and permanent magnet synchronous machine (PMSM), and proposes to apply the machine in robotic transmission system.

Cycloid gear drive is a transmission device that is commonly used to boost up the output torque. It has been widely applied in many industrial applications including ship power transmission, robotic actuation, hybrid electric vehicle and renewable energy due to advantages of high mechanical efficiency, low backlash, compact size and high ratio mechanical transmission. The structure of cycloid gear is different from common gears which engage externally, it engages internally and operates in cycloidal motion. In robotic

industry, requirements on compact size and high transmission ratio result in the application of cycloid gear drives. Chapter 2 would introduce it in detail.

Synchronous electric machine has been widely applied and investigated for more than a century. In industry, synchronous machines are used for power generating, electric power drive and many other electro-mechanical transformations. In particular, permanent magnet synchronous machine (PMSM) is the most common one because the control strategy is relatively simple with the help of booming power electronics. Commonly, PMSM is used as mechanical power input in robotic industry. Chapter 3 would elaborate it.

Typical human-sized legged locomotion needs an output torque around 300 N·m to accomplish motions. The direct drive design uses only one high-torque electric machine with multi-stage transmission cannot meet the size and weight requirement of the leg actuation. This research proposes a novel cycloid electric machine to replace the conventional motor transmission system. An estimated 40 percent size and weight reduction is expected [19].

High Torque Density Cycloid Electric Machines for Robotic Application

by

Rui Liu

A THESIS

submitted to

Oregon State University

In partial fulfillment of
the requirements for the
degree of

Master of Science

Presented June 7, 2017
Commencement June 2018

Master of Science thesis of Rui Liu presented on June 7, 2017.

APPROVED:

Major Professor, representing Electrical and Computer Engineering

Director of the School of Electrical Engineering and Computer Science

Dean of the Graduate School

I understand that my thesis will become part of the permanent collection of Oregon State University libraries. My signature below authorizes release of my thesis to any reader upon request.

Rui Liu, Author

ACKNOWLEDGEMENTS

Foremost, I would like to express my deep gratitude to my thesis adviser Dr. Julia Zhang who expertly guided me and shared the valuable advice with me in the past year. Her unwavering enthusiasm and abundant academic experiences motivated me to explore the researches. I will never forget her high academic standard and patience in teaching which directed me to solve problems in the academic. It is her that offered me a chance to approach academic researches and encouraged me in the study. I am lucky to be her student.

I would also extend my appreciations to Dr. Ted Brekken, Dr. Eduado Cotilla-Sanchez and Dr. Annette von Jouanne who have made great contributions to our energy system community, and who have built an admirable academic environment for our colleges' faculties and students. In addition, I would like to thank Xiong Han for guiding me on software and providing me pertinent suggestions. I learned a lot ever time when I discussed with him. My gratitude also goes to my graduation council representative Dr. Leonard Coop who has offered valuable feedbacks on my research. I am also grateful for Dr. Johnathan Hurst and his Ph.D. student Andrew M Abate. Their generous help facilitated my learning on cycloid gears.

I am also indebted to my friends and all energy group members in the Dearborn basement. Xiao yang, Yanyan Xie, Peng Peng, Ian Fox, Colin Quinn Comard etc. I am always

delighted when I stay with yours. The time I spent with yours will be the memory that I treasure the most.

Finally, I would like to thank my parents in China, they have supported me through my entire life abroad. My love for them have been accumulated with the time goes on. I may be the greatest gift in their eyes, but now they are the greatest gift in my life. Here I express my great gratitude to them.

At the very end, I would like to remind myself to keep striving in the future, only the persistence and courage will lead me to the accomplishment.

TABLE OF CONTENTS

TABLE OF CONTENTS (Continued)

Page

LIST OF FIGURES

Figure Page

LIST OF FIGURES (Continued)

Figure Page

LIST OF TABLES

Table Page

Chapter 1 : Introduction

1.1 Motivation

Recent years, cycloid gear transmission has drawn the attention of both industry and academia. The dominate component in this transmission system is termed cycloid gear. Typically, cycloid gears are often used as speed reducer/amplifier. According to the cycloid gears' geometry, it has many outstanding advantages than other gears, such as: it is a single stage reduction device with a wide range of reduction, big kinematical (reduction/amplifier) ratio, high mechanical efficiency, compact size and weight and low reflective inertia [1,2,4]. Due to those remarkable advantages, cycloid gear can be used in many industrial fields such as boats, hybrid vehicle, pumps, robot arm joints, medical equipment and hydro and wind renewable energy [5].

Alternating current (AC) electric machines have been applied and investigated for centuries, along with developed and various control strategies, electric machines have been used in a wide range of industry fields. From hybrid vehicles and hypo power generators to space aircraft, electrical machines never stop to generate and convert power for humans. Generally, electric machines can be classified into three types: electric motors, electric generators and transformers. The most widely used machine is the electric motor, which turns electric energy into mechanical energy. In electric motors, synchronous machines and induction machines are most commonly applied in industry. Due to the innovation of

semiconductors, magnetic materials and control theory, and also because of advantages such as compact size, higher efficiency, big power factor and relatively simple structure, synchronous machines are more widely used than another types of electric AC machines.

As introduced above, cycloid gears are able to transmit power and synchronous electric machines can covert power, the integration of both becomes an inevitable tendency in industry, such as transportation driving system. Meanwhile, robotic technology gains increasing popularity in the past decades, and robots' complex motion requires the integration of both mechanical transmission system and electric power supply. Therefore, mechatronic transmission system is imposed on robotic industry [4]. Rely on advanced technologies and materials, high power density, high efficiency and compact size and weight are required in future robotic industry. For example, a typical human-sized legged locomotion needs about 300 $N \cdot m$ torque. Normally, engineers use the multi-stage gearbox to boost up torque from input side to output end. However, the complex bulky gearbox results in increased weight and reduced efficiency. In order to reduce the size and weight and acquire high torque density, a novel machine is proposed in this thesis---a cycloid electric machine which combines cycloid gear and electric motor. An estimated 40% size and weight reduction is expected [19]. Details are in following chapters.

1.2 Literature Review

This proposed machine combines cycloid gear and electric motor, and it would be applied in robotic locomotion system. The whole structure of this machine is similar to cycloid gear, but some coils are added to the ring gear which is similar to the coil distribution in the electric machine stator. As cycloid gears are gradually used in industry fields, many contributions have been made by researchers. Cycloidal lantern gear transmission would be the earliest industrial application of cycloid gear, however, it has many disadvantages such as low efficiency. In the 1990s, Shen published a United States Patent, and it presents an early prototype of modern cycloid gear transmission [11]. While manufacturing a cycloid gear, however, is not easy because of the special cycloidal tooth (or lobe) profile. To solve this problem, Shin and Kwon classified cycloid gears based on the gear profile and ring gear motion. Moreover, the greatest contribution they made was deriving the general profile equations based on Kennedy's theorem [25-27]. On this basis, and in accordance with the application, researchers started to design modern cycloid gear transmission. Hwang and Hsieh investigated different geometry of cycloid gears between gerotors and speed reducers, and they also determine gear profile which may prevent undercut [8, 12]. Neagoe and Diaconescu modified the gear structure to get higher kinematic ratio and claim that it can be applied in renewable energy system as a speed reducer [5]. Demenego and Vecchiato focus their researches on designing cycloid gear pump, they investigate the geometry of cycloid gear pump and simulate their design [6,

14]. Choi and Kim's group also modified the rotor gear profile for the cycloid pump, and their research eliminates the upper limit on the eccentricity, in this case, undercut is avoided [3]. Other than being applied as a pump, cycloid gears are gradually used in robots design in recent years. Shao and Wang proposed a new two-stage cycloid transmission used in robot joint system, and they claim the transmission ratio can reach 5 to 10 times the conventional cycloid transmission [21]. Song and Liao presented a new cycloid-like profile transmission device, but the experimental results do not match with simulation results, therefore their prototype needs to be modified [20]. However, cycloid gear structures described above do not incorporate any component which is able to provide electromagnetic torque. Some papers propose cycloid permanent magnetic gear which uses mounted magnets performed like gear teeth. Although the experimental results are inspiring, they are still in exploratory stage [16, 17]. In this thesis, a new cycloid electric machine is proposed. Based on the cycloid gear structure, electromagnetic torque is integrated to enhance the output torque. This thesis only discusses the design of the cycloid machine structure and the feasibility for its application. The controls of such machine will be investigated in future work. Therefore, the author separately introduces two basic devices which would be combined together. Then, build the prototype in SolidWorks and simulation model in ANSYS, and finally analyze the simulation results.

1.3 Chapter Review

Chapters in this thesis are organized in a logic sequence illustrated in Figure 1.1.

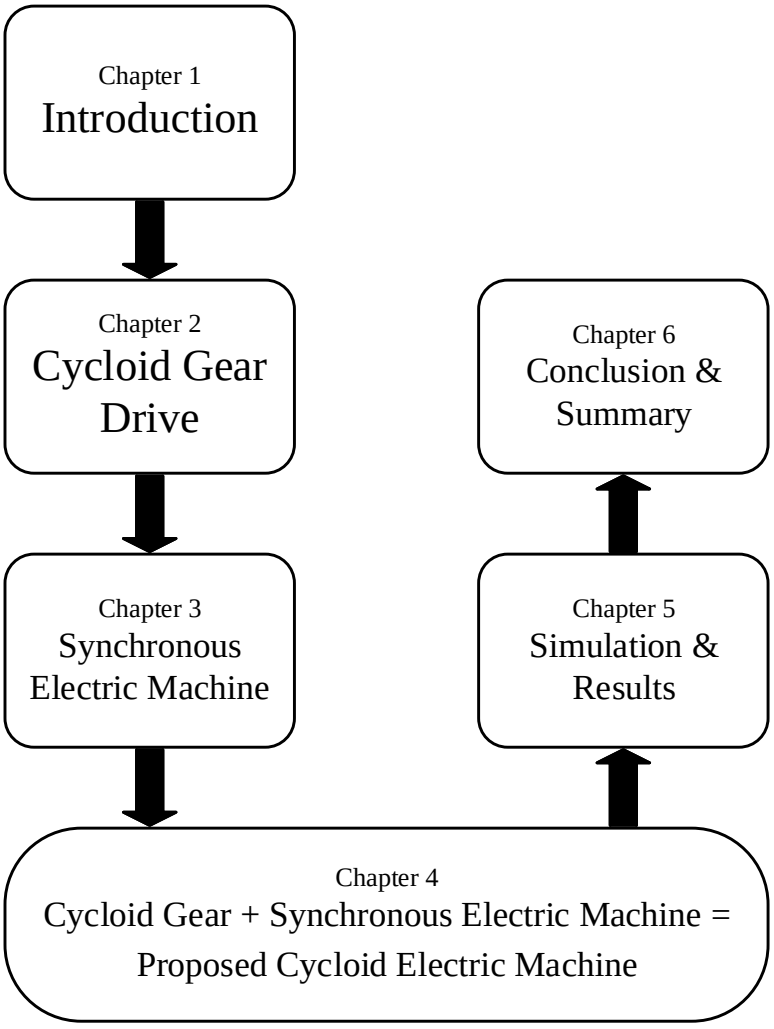

Figure 1.1 Chapters Distribution.

Chapter 2 generally introduces the cycloid gears including geometry, operating principle, and application. In geometry section, it illustrates the referenced gear geometry, and the geometry mathematical basis; in the operating section, it presents the gear eccentric rotation, and based on the rotation, deduce the gear ratio related to torque transfer. The last section lists the gears' applications in industry.

Chapter 3 replicates the logic sequence of chapter 2, but targets to different object---synchronous electric machine. In geometry introduction section, it introduces the referenced motor structure and subcomponent’s function; in the operating section, it illustrates the relation between permanent magnets and electromagnetic field, and how the rotational magnetic field lead rotor to rotate.

Chapter 4 presents the proposed cycloid electric machine. It demonstrates the machine's geometry in detail. Operating principle section introduces details of how magnetic field would result in a cycloidal rotation under ideal conditions. By understanding the operating principle, the possible application is discussed in the application section. At the moment, chapter 4 gives a perceptual understanding of the machine.

In chapter 5, the author explains the process of simulation in detail. First two sections introduce machine structure modeling in SolidWorks, and the model is then exported to ANSYS for drawing windings and doing finite element analysis. In the result section, the author presents simulation results and analyzes the feasibility.

In the last chapter 6, progress would be summarized and conclusions drawn. The last chapter will also introduce the future work for this research.

Chapter 2 : Cycloid Gear Drive

According to Shin and Kwon [1], cycloid gear drives can be classified into four types: stationary ring gear epicycloid gear drive, rotating ring gear epicycloid gear drive, stationary ring gear hypocycloid gear drive, and rotating ring gear hypocycloid gear drive. In the proposal, stationary ring gear epicycloid gear drive would be applied.

2.1 Cycloid Gear Structure.

The common stationary ring gear type epicycloid gear drive includes three main parts: the input shaft including eccentric cam, cycloid gear box, and output shaft (see Fig 2.1). The cycloid gear box comprises the cycloid disk which is the rotating part, and the ring gear (or ring gear rollers) which is the stationary part. (In practice, the ring gear shape can be classified into two types: one is shown in Figure 2.1 which is constructed by rollers; the other type is shown in Figure 2.2 whose ring gear looks like a plate, and which would be applied in this thesis and details would be described in later chapters.) The output shaft contains a metal plate and output pins (see Figure 2.1 or Figure 2.2). To assemble those components, the eccentric cam would be inserted into the central hole of the cycloid disk, ring gear rollers are located in a fixed housing and the four output pins would be inserted into the four distributed holes in the cycloid disk to transmit the torque. Detailed operating principles would be introduced in section 2.2.

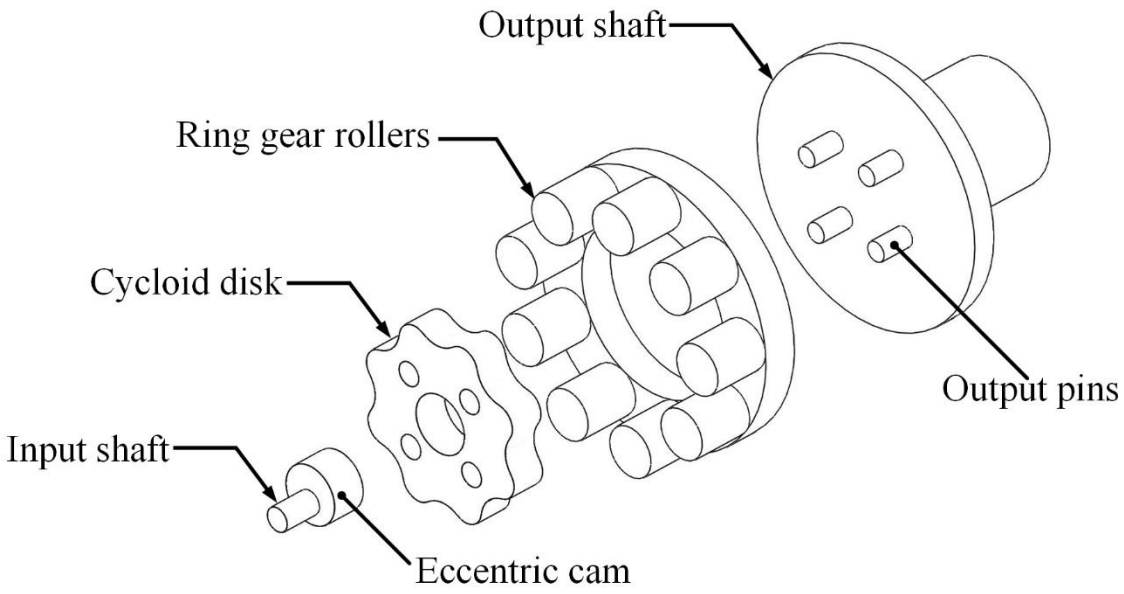

Figure 2.1 Typical cycloid gear set A

.

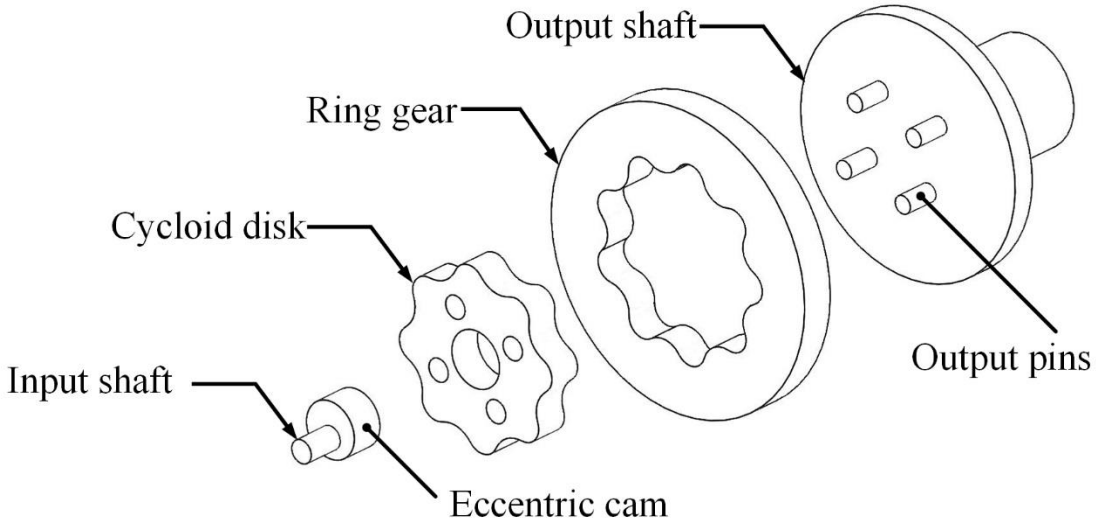

Figure 2.2 Typical cycloid gear set B

2.1.1 Introduction of Epicycloid Curve and Hypocycloid Curve

The core component in the cycloid drive is cycloid disk, and the cycloid disk tooth (or called lobe hereinafter) profile is drawn by two curves: epicycloid curve and hypocycloid curve. While the ring gear tooth profile is derived either from the location of rollers or the sweep trajectory formed by the eccentric rotation of the cycloid disk.

The cycloid curve is the locus of a fixed point on the rim of a generating circle which rolls align with the base line without slippage. An epicycloid curve is a kind of cycloid curve whose generating circle rolls outside along the base circle. Figure 2.2 illustrates the epicycloid curve generation. On the contrary, a hypocycloid curve is a kind of cycloid curve whose generating circle rolls inside along the base circle.

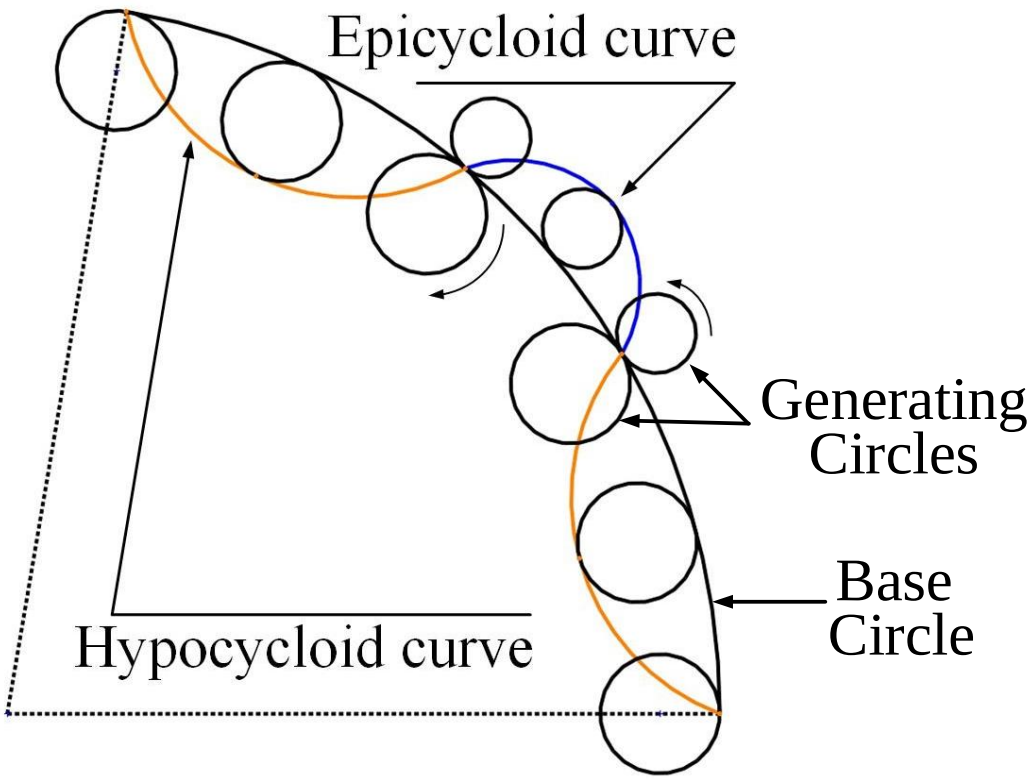

Figure 2.3 Cycloid disk profile derived from epicycloid curve and hypocycloid curve.

According to the figure above, it reveals that the radius of generating circle determines the width of the lobe. When the rolling circle's radius becomes bigger, the route swept by rim point on the circle is longer which means the lobe is bigger.

2.1.2 Cycloid Disk Tooth Profile and Ring Gear Tooth Profile

Based on the concept of epicycloid and hypocycloid curves, and according to Kennedy's instant velocity center theorem [25-27], both cycloid disk profile and ring gear shape would be acquired by calculation. However, Shin and Kwon's paper [1] summarized the theorem and derived the cycloid disk profile equations as below:

$$C_{\mathrm{x}} = R\cos\emptyset - R_{\mathrm{r}}\cos(\emptyset + \varphi) - E\cos(N\emptyset) \qquad \text{Equation 2.1}$$

$$C_{\mathrm{y}} = -R\cos\emptyset + R_{\mathrm{r}}\cos(\emptyset + \varphi) + E\cos(N\emptyset) \qquad \text{Equation 2.2}$$

$$\varphi = \tan^{-1}\left[\frac{\sin[(1-N)\emptyset]}{(R/EN)-\cos[(1-N)\emptyset]}\right] \quad (0^{\circ} \le \emptyset \le 360^{\circ}) \qquad \text{Equation 2.3}$$

where: R is the distance from ring gear center to roller position center, $\emptyset$ is the input shaft rotate angle, φ is the contact angle, R_r is the ring roller radius, N represents the number of roller and E equals to the eccentricity value. In this paper, R=46.2 mm, R_r=10.5mm, N=9, E=3.2mm are chosen. Note that $\emptyset$ is a variable from 0-2π.

Based on Equations 2.1 to 2.3, the cycloid disk profile can be obtained. Figure 2.4 (a) shows the cycloid disk tooth profile derived from above parameters and equations. As the radius of ring gear R and roller radius R_r is known, the ring gear profile is drawn according to these two parameters. Figure 2.4 (b) indicates the ring gear roller distribution and ring gear tooth profile derived from rollers.

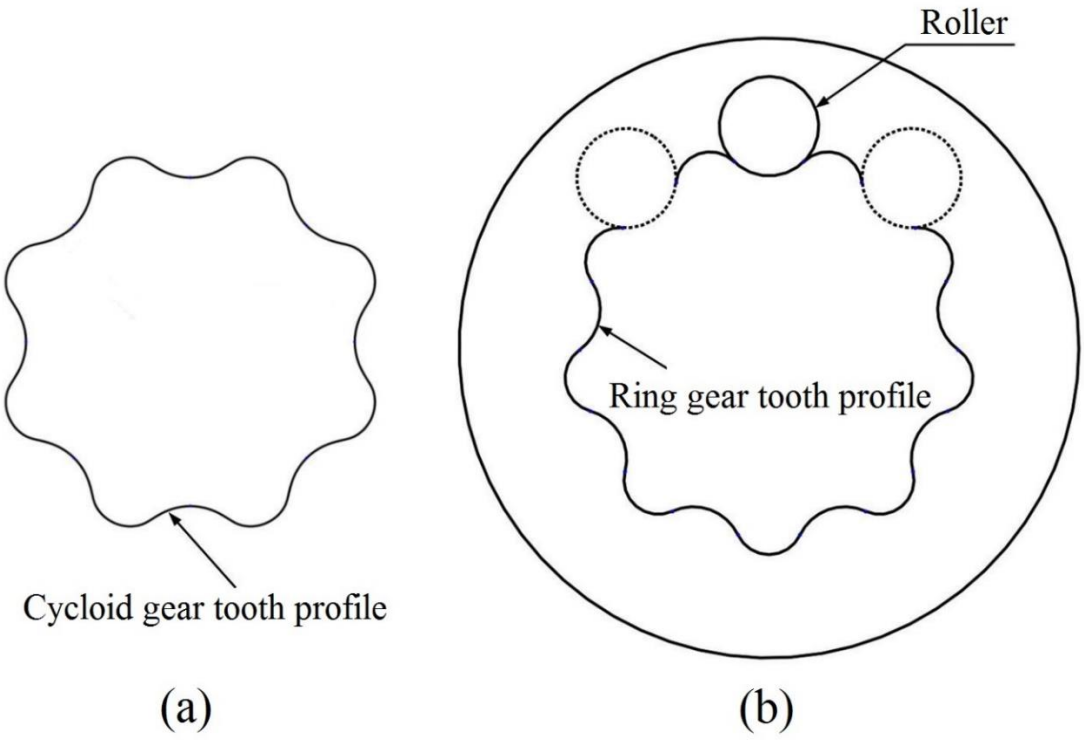

Figure 2.4 Cycloid gear tooth profile. (a) Cycloid disk profile, (b) ring gear profile derived from rollers location.

2.2 Cycloid Gear Operating Principle

2.2.1 Gear Ratio

The cycloid gear is often used as a speed reducer, and the tooth number difference between cycloid disk and ring gear is one. Ideally, the mechanical transmission efficiency is assumed to be100%, we have this relationship:

$$T_{\text{in}} G_{\text{ratio}} = T_{\text{out}} \qquad \text{Equation 2.4}$$

where: T_{in} is the torque provided by the input shaft, and T_{out} is the output torque, G_{ratio} refers to the mechanical ratio (gear ratio).

Similar to other type of gears, the cycloid gear's gear ratio is defined by tooth number and operating principle. Following is a general introduction of the gear ratio derivation. Based on the special structure of cycloid gears, when the input shaft takes one revolution, the cycloid disk takes $1/L$ revolution (L is the number of lobes on the cycloid gear) in the opposite direction, which means the speed reduction ratio is -L which is the gear ratio (details would be illustrated in section 2.2.2). Then the relationship can be written as:

$$T_{\text{in}}(-L) = T_{\text{out}} \qquad \text{Equation 2.5}$$

where: L is the number of rollers or number of lobes on the cycloid disk. ($L > 1$)

Equation 2.5 is the torque transmission equation for cycloid gear, and it also indicates that the input torque and output torque are in opposite directions.

2.2.2 Operating Principle

The cycloid gear is also a kind of plenary gear, so that the cycloid disk has both revolution and rotation. The revolution center coincides with the ring gear center, but the rotation center coincides with the cycloid disk center. This two geometric centers are misalign. The input shaft forces the eccentric cam to do eccentric rotation, which generates a force to push the cycloid disk against ring gear. With the engagement of ring gear teeth (gaps or pins), the cycloid disk starts to rotate lobe by lobe. This motion is similar to that a wheel rolls around the inner side of a circle. When the wheel rolls on the inner side of the circle, it turns on its own rotating center in an opposite direction [1]. Generally, the tooth (lobe) number on the cycloid disk is one less than the tooth (gap) number on the ring gear. This one tooth difference results to the mechanical ratio. As introduced in section 2.2.1, the input shaft turns one revolution, the cycloid disk rotates $1/L$ revolution in the opposite direction. Correspondingly, the speed reduction ratio equals to $-L$. Figure 2.5 indicates this operating principle.

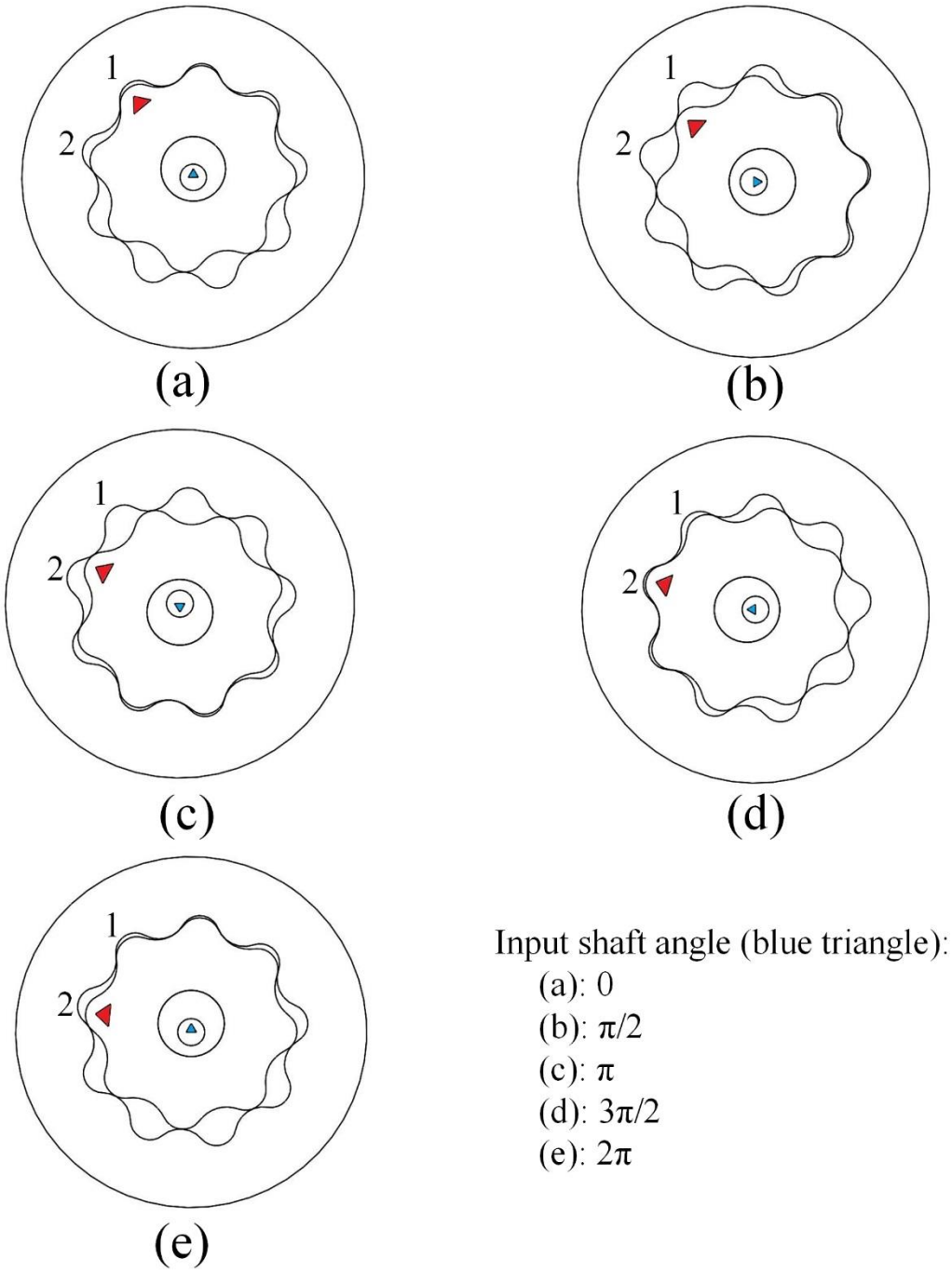

Figure 2.5 Cycloid gear operation

In the Figure 2.5, the blue triangle represents the input shaft, and the red triangle represents one lobe of cycloid disk. When the cycloid disk lobe transfers from ring gear gap 1 to gap 2, the input shaft turns 2π clockwise, while the disk lobe turns $2\pi/L$ (Here L=8) counterclockwise as introduced above. Apparently, the speed is reduced to $\frac{1}{-L}$ which equals to the gear ratio.

According to the law of conservation of energy, the output torque would be amplified as the output speed is reduced. To transmit the increased torque to output end, there are several pins on the output shaft plate, and those pins would be inserted into corresponding holes in the cycloid disk as shown in Figure 2.1. Those holes push output pins to drive the plate and produce the increased output torque.

2.3 Application Field

Cycloid gear drive has been found advantages such as light weight, compact size, low noise, high gear ratio, highly precise gear reduction and high mechanical efficiency [1-5]. Conventionally, cycloid gear drive is designed to be an internal gear pump which is also termed a gerotor. It can be used in boats' oil transmission [4]; in hybrid vehicles, this cycloidal pump is also used to shut or start the engine [3]. Recently, as the robotic industry is booming, designers attend to take advantages of cycloid gears on its speed reduction performance. For instance, cranes, the mechatronic system in renewable energy (amplifier in hydro and wind system) [5], a reduction transmission for an actuator in a robot joint

drive [7]. To date, a commercial cycloid gear product named RV reduction gear has come into use in industrial robots. Nabtesco which is the manufacturer of this high-performance reduction gear, clams that this product now has been used across a wide range of industries. Product features are in the appendices.

Chapter 3 : Permanent Magnet Synchronous Machine (PMSM)

The synchronous electric machine is able to convert electric energy to mechanical energy or vice versa. It is a most widely used alternating current (AC) machine. The phrase synchronous machine implies that the rotor speed is proportional to the stator current frequency. Due to this character, synchronous machines are suitable for workplaces which require constant speed, such as turbine generator and hydroelectric generator. Also, the ability of adjusting power factor allow them to be power supplies for the power system. With the booming electronic technology, permanent magnet synchronous machines (PMSM in short) are applied extensively in variable speed drives [24].

Because of the research stage, the PMSM control strategy would not be discussed in this thesis.

3.1 Permanent Magnet Synchronous Machine Geometry

Generally, permanent magnet synchronous machines are constructed with two basic components: the rotor and the stator. In the stator, windings or coils are inserted in slots distributed in the lamination. These windings are used to carry AC currents which would generate rotating magnetic fields to pull the rotor to turn. In order to generate constant magnitude and constant speed rotating magnetic field, windings should be distributed symmetrically in uniform stator slots. Correspondingly, the rotor has permanent magnets

which would be coupled with magnetic field poles generated by stator windings. Note that Rotor magnets can be distributed either in the rotor or on the rotor surface.

This section introduces the stator and the rotor structure so that the machine operating principle would be better understood in the next section. Figure 3.1 illustrates a simple 2 poles round rotor PMSM. Rotor magnets are embedded in the rotor.

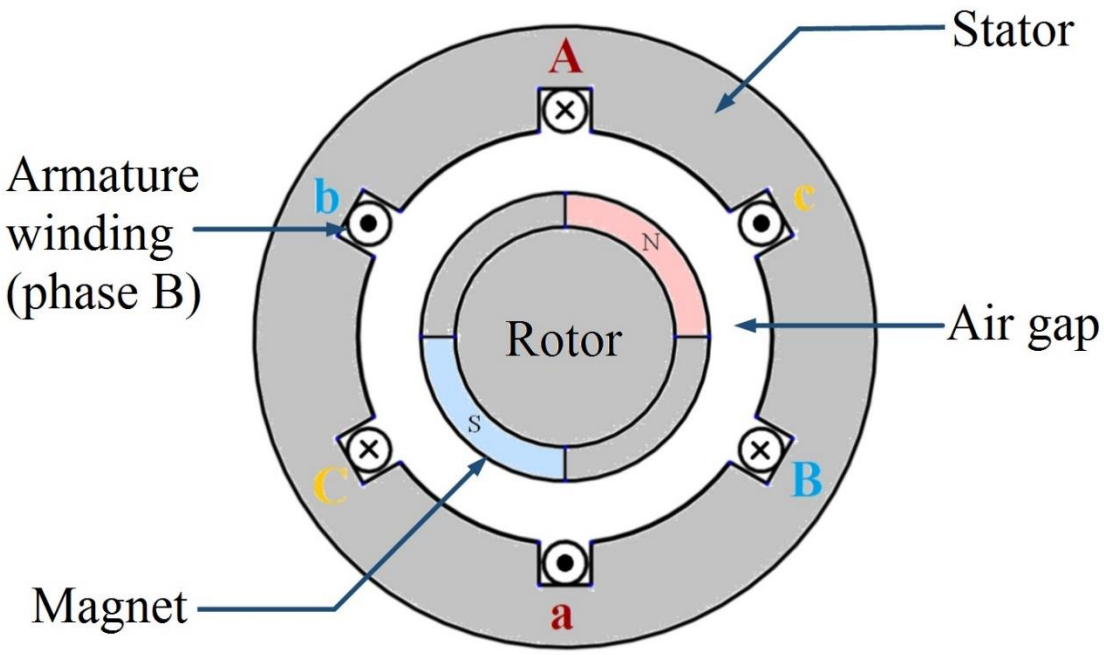

Figure 3.1 Two poles, round rotor permanent magnet synchronous machine.

From the figure above, windings are distributed in the stator lamination. Due to alternating current carried in windings, a resultant flux would start to rotate in the air gap. This phenomenon would be expatiated in the next section. Meanwhile, the resultant flux generates two poles which are the North Pole and the South Pole, while magnets on the rotor would be attracted by them, so the stator electric field would lock the rotor and force it to rotate at the synchronous speed.

3.2 Permanent Magnet Synchronous Machine Operating Principle

In this section, the author introduces the operating principle in two subsections: rotating magnetic field and machine operation.

3.2.1 Rotating Magnetic Field

Rotating magnetic field is the core factor of PMSM which drives the rotor to spin. As introduced, the rotating magnetic field locks rotor magnets and lead them to spin. It can be obtained from the multi-phase current carried in distributed stator windings, normally, it applies three-phase current. To illustrate this phenomenon, a single phase model is created to conduct the derivation, shown in Figure 3.2 [24]

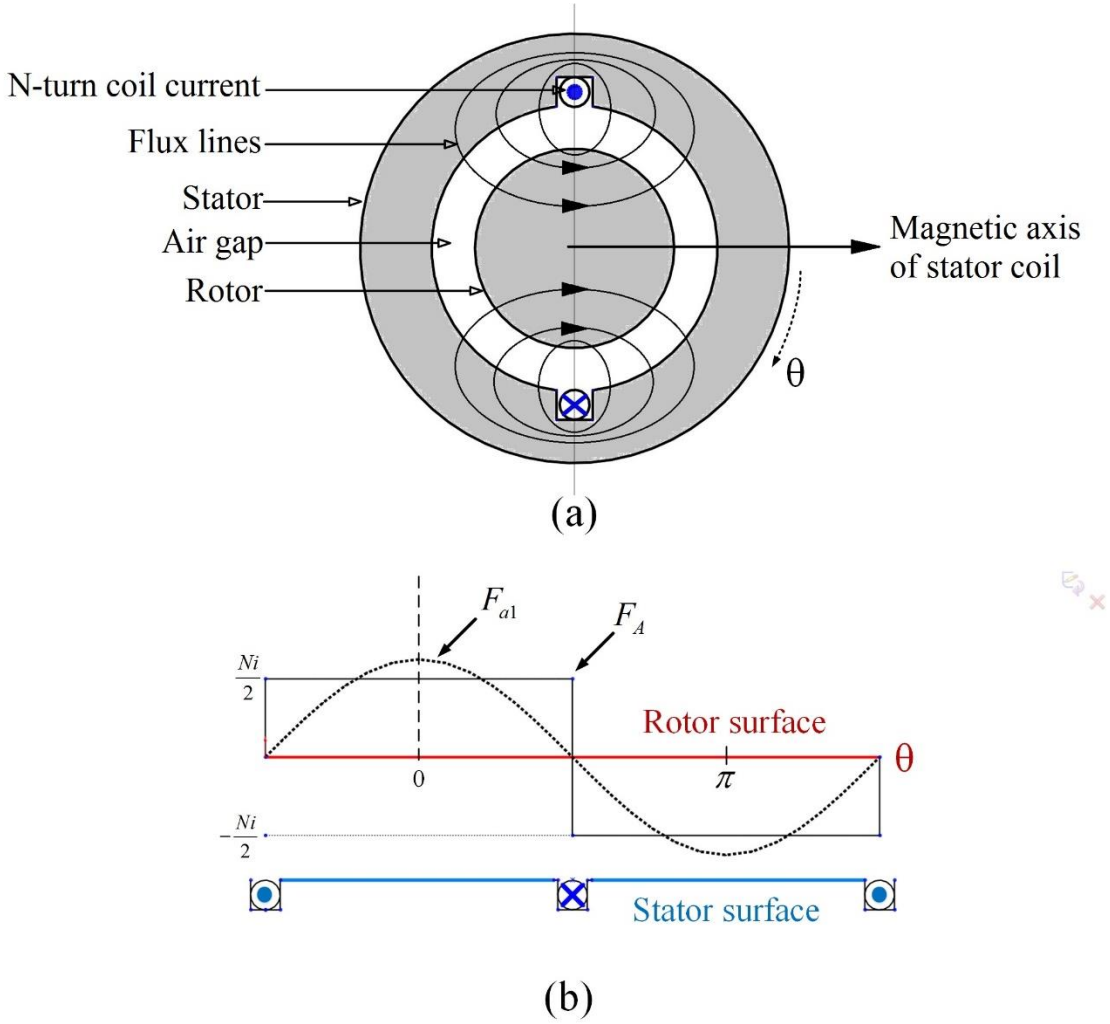

Figure 3.2 Single phase machine model and approximate magnetomotive force (MMF) distribution.

The figure indicates that the single phase winding generates a two poles magnetic field, according to right-hand screw rule, the field direction is shown as magnetic axis in

the Figure 3.2 (a). Assuming that the MMF generated by winding is equal to F_{A}, and the air gap is uniform, the MMF would be consumed evenly by two sections of air gap which mean in each air section, it consumes $\frac{1}{2} \times F_{\mathrm{A}}$ at any time. This assumption makes F_{A} become a square wave shown in Figure 3.2 (b), and in terms of Ampere circular theorem:

$$F_{\mathrm{a1}} = \frac{1}{2} F_{\mathrm{A}} = \frac{1}{2} Ni \qquad \text{Equation 3.1}$$

where: F_{a1} is MMF consumed in air gap section, N is the number of turns of winding, i is the winding current.

Applying Fourier Series analysis on the square wave and obtain the fundamental component:

$$F_{\mathrm{a1}} = \frac{4}{\pi} \frac{Ni}{2} \cos\theta \qquad \text{Equation 3.2}$$

where: θ is the electrical angle displacement from the magnetic axis shown in Figure 3.2.

Now, assuming winding current $i = I_{\mathrm{m}} \cos\omega t$ and substitute it into Equation 3.2, then rewrite equation:

$$F_{\mathrm{a1}} = F_{\mathrm{m}} I_{\mathrm{m}} \cos\omega t \cos\theta \qquad \text{Equation 3.3}$$

The coefficient $F_{\mathrm{m}}I_{\mathrm{m}}$ is the amplitude of fundamental component, in order to obtain the accurate value of F_{m}, the winding distribution must be taken into consideration. According to reference [24].

$$F_{\mathrm{m}} = \frac{4}{\pi}\frac{k_{\mathrm{w}}N_{\mathrm{per-phase}}}{P} \qquad \text{Equation 3.4}$$

Where: k_{w} is a constant termed winding factor, $N_{\mathrm{per-phase}}$ is the number of turns per winding, P is the number of poles. Now write done all three phase fundamental MMF expression:

$$F_{\mathrm{a1}} = F_{\mathrm{m}}I_{\mathrm{m}}\cos\omega t\cos\theta \qquad \text{Equation 3.5}$$

$$F_{\mathrm{b1}} = F_{\mathrm{m}}I_{\mathrm{m}}\cos(\omega t - \frac{2\pi}{3})\cos(\theta - \frac{2\pi}{3}) \qquad \text{Equation 3.6}$$

$$F_{\mathrm{c1}} = F_{\mathrm{m}}I_{\mathrm{m}}\cos(\omega t + \frac{2\pi}{3})\cos(\theta + \frac{2\pi}{3}) \qquad \text{Equation 3.7}$$

To obtain the resultant MMF, above three equations must be factorized. In terms of the mathematical rule:

$$\cos\alpha\cos\beta = \frac{1}{2}[\cos(\alpha+\beta) + \cos(\alpha-\beta)] \qquad \text{Equation 3.8}$$

Then Equations 3.5-3.7 are changed to:

$$F_{a1} = \frac{F_m I_m}{2}[\cos(\omega t + \theta) + \cos(\omega t - \theta)] \quad \text{Equation 3.9}$$

$$F_{b1} = \frac{F_m I_m}{2}[\cos\left(\omega t + \theta - \frac{4\pi}{3}\right) + \cos(\omega t - \theta)] \quad \text{Equation 3.10}$$

$$F_{b1} = \frac{F_m I_m}{2}[\cos\left(\omega t + \theta + \frac{4\pi}{3}\right) + \cos(\omega t - \theta)] \quad \text{Equation 3.11}$$

Apparently, the sum of $F_{a1}, F_{b1}\ and\ F_{c1}$ is:

$$F_1 = \frac{3}{2} F_m I_m \cos(\omega t - \theta) \quad \text{Equation 3.12}$$

Because:

$$\cos(\omega t + \theta) + \cos\left(\omega t + \theta - \frac{4\pi}{3}\right) + \cos\left(\omega t + \theta + \frac{4\pi}{3}\right) = 0 \quad \text{Equation 3.13}$$

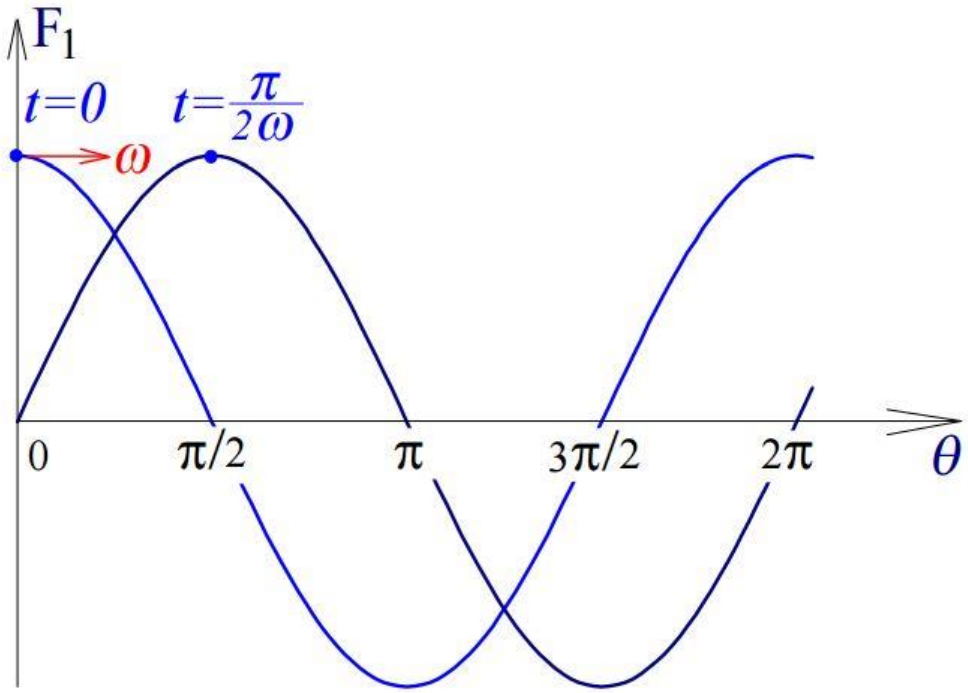

Figure 3.3 Resultant MMF travelling diagram.

From Equation (3.12), it can be indicated that the resultant MMF is a function of time and electric displacement. It means, at a certain location in the air gap, the MMF amplitude varies with time as a cosinusoidal wave. Figure 3.3 presents the waveform of resultant MMF, and it indicates that resultant MMF is a traveling wave with electric angular speed:

$$\omega_{\mathrm{e}} = \frac{\theta}{t} = \omega \quad \text{(rad/s)} \qquad \text{Equation 3.14}$$

Equation 3.14 reveals the MMF traveling electric speed ω_e is equal to winding current's angular frequency ω. However, this is an electric speed which means the angle between two adjacent opposite poles is 2π instead of the physical circle angle. Therefore, poles number should be taken into consideration when deriving the mechanical speed:

$$\omega_m = \frac{\omega_e}{P/2}\ (\text{rad/s}) = \frac{60\omega_e}{P\pi}\ (\text{rpm}) \qquad \text{Equation 3.15}$$

where P is the number of designed poles.

Above derivation reveals the rotation of MMF, and it indicates that the PMSM rotor speed depends on two factors: winding current electric angular frequency and machine poles number defined by winding distribution. Other than mathematical derivation of rotational MMF, a series of diagrams may also help readers to understand the rotating MMF principle. Figure 3.4 displays the relationship between current phase and MMF space position.

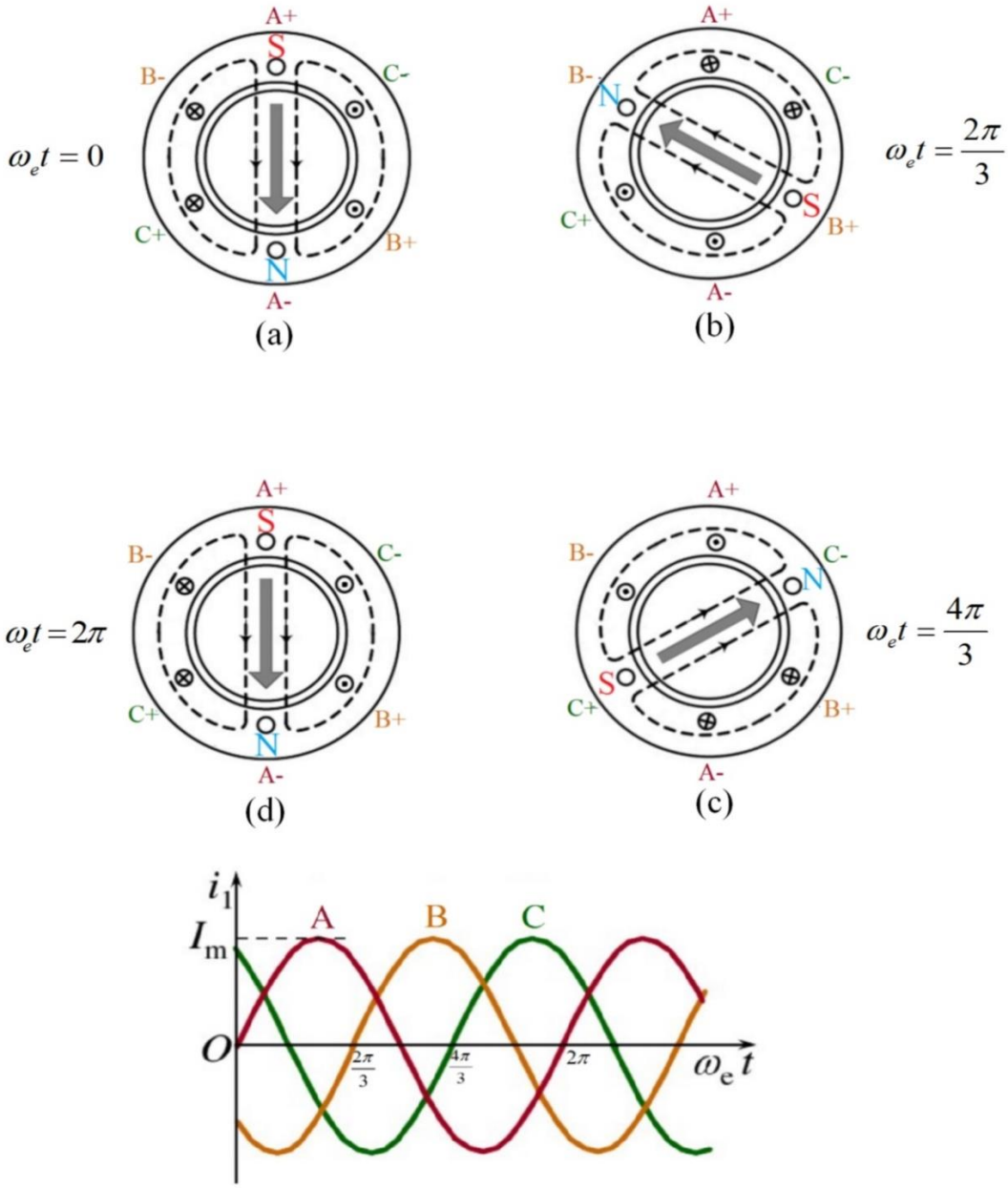

Figure 3.4 Three-phase two poles winding generates rotational MMF.

3.2.2 Machine Operation.

Based on the rotating magnetic field, machine operating principle can be understood easily. When stator windings generating rotating magnetic field which is shown in Figure 3.4, magnets embedded on the rotor will be locked in the corresponding field pole. Therefore, the rotor would follow the rotating magnetic field at the synchronous speed.

However, permanent magnet synchronous machines have an evident disadvantage: the machine cannot start at synchronized speed because of the rotor inertia and the load [24]. When starting the machine, the rotating field immediately reaches the synchronous speed. Yet, the speed is too fast for the stationary rotor to catch up, which means rotating field poles cannot lock rotor magnets. In practice, this problem can be solved by embedding copper or aluminum material squirrel-cage shape close circuit in the rotor and the machine is able to start as induction machines. At present, thanks to power electronic inverter, this problem can be perfectly solved by adjusting stator current frequency from low to synchronous value.

Chapter 4 : Proposed Device—Cycloid Electrical Machine

The proposed device is an integration of cycloid gear and synchronous electric machine. The whole structure is similar to Figure 2.3, the modifications are on the cycloid gear set including the ring gear and cycloid disk. According to the proposal, the ring gear will have armature windings on it, and permanent magnets will be inserted in the cycloid disk. In this case, an 8 poles electrical machine would be formed, and it would produce electromagnetic torque to enhance the output torque density.

4.1 Geometry of Cycloid Electrical Machine

The whole structure of the proposed cycloid electrical machine is based on the cycloid gear drive geometry introduced in chapter 2. Nevertheless, the cycloid gear part is modified to a cycloid electric gear. Generally, it has two main components: the cycloid disk (the rotor), and the ring gear with coils (the stator). Following sections would illustrate modified details on these two components.

A geometry overview is shown in figure 4.1, it demonstrates the two main components of the machine.

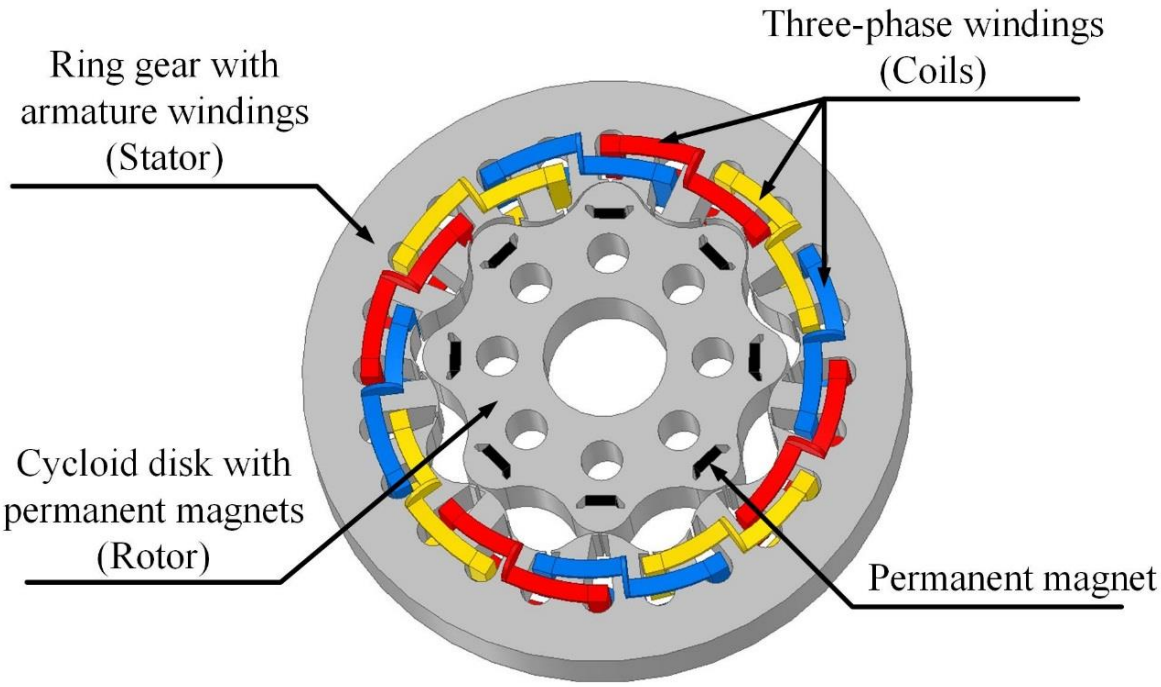

Figure 4.1 Cycloid electric machine geometry overview.

4.1.1 Cycloid Disk Rotor

For the internal cycloid disk rotor (rotor in short), the profile is the same as the cycloid disk according to the same drawing equations introduced in chapter 2. However, in order to couple the electromagnetic field generated in the stator, several permanent magnets are inserted in the rotor's lobes. In accordance with the rotor geometry, there are eight lobes on

the rotor. To make magnets distribute evenly and to make it operates more like a motor, the author designs one magnet per lobe, which means eight poles for the machine. Figure 4.1.1 indicates the magnets distribution and polar distribution on the rotor.

Based on profile generation equations introduced in chapter 2, the rotor shape is built in Figure 4.2. Moreover, magnets are inserted in the lobes.

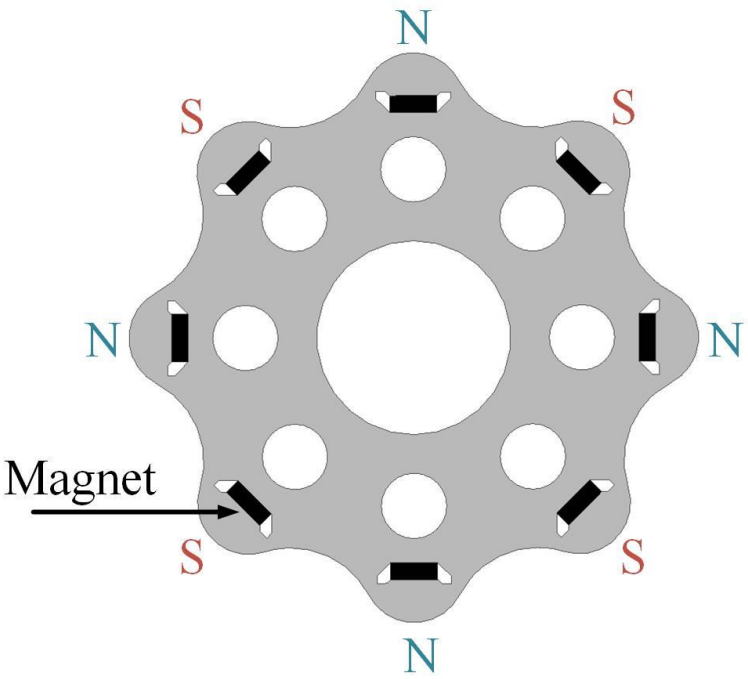

Figure 4.2 Cycloid disk rotor with magnets top view.

4.1.2 Ring Gear Stator

The stator shape of the proposed machine is based on the cycloid ring gear, but the geometry is modified to adapt coils which produce an electromagnetic field to drive the magnetic rotor. In order to add coils in the stator, several slots are designed. As referred in 4.1.1, the machine has eight poles, and suppose to use three phase current to generate electromagnetic poles, so the number of slots is calculated as 24. According to ANSYS IPM motor tutorial [23], the author distributes those 24 slots evenly around the pitch circle of the ring gear. Figure 4.3 presents the ring gear geometry with 24 slots and indicates the pitch circle.

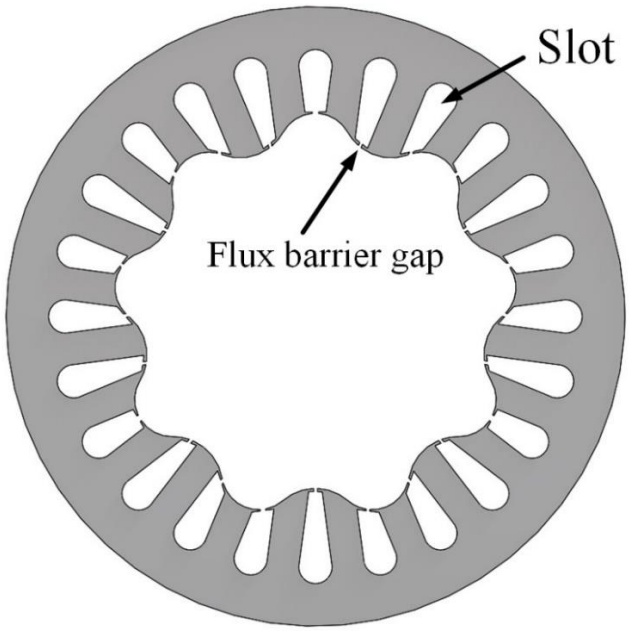

Figure 4.3 Ring gear geometry with coil slots.

Current coils in the stator are used to produce rotating electromagnetic field, while they must be distributed in a specific law so that the magnetic field is able to rotate. Figure 4.4 reveals the coil distribution in the slots.

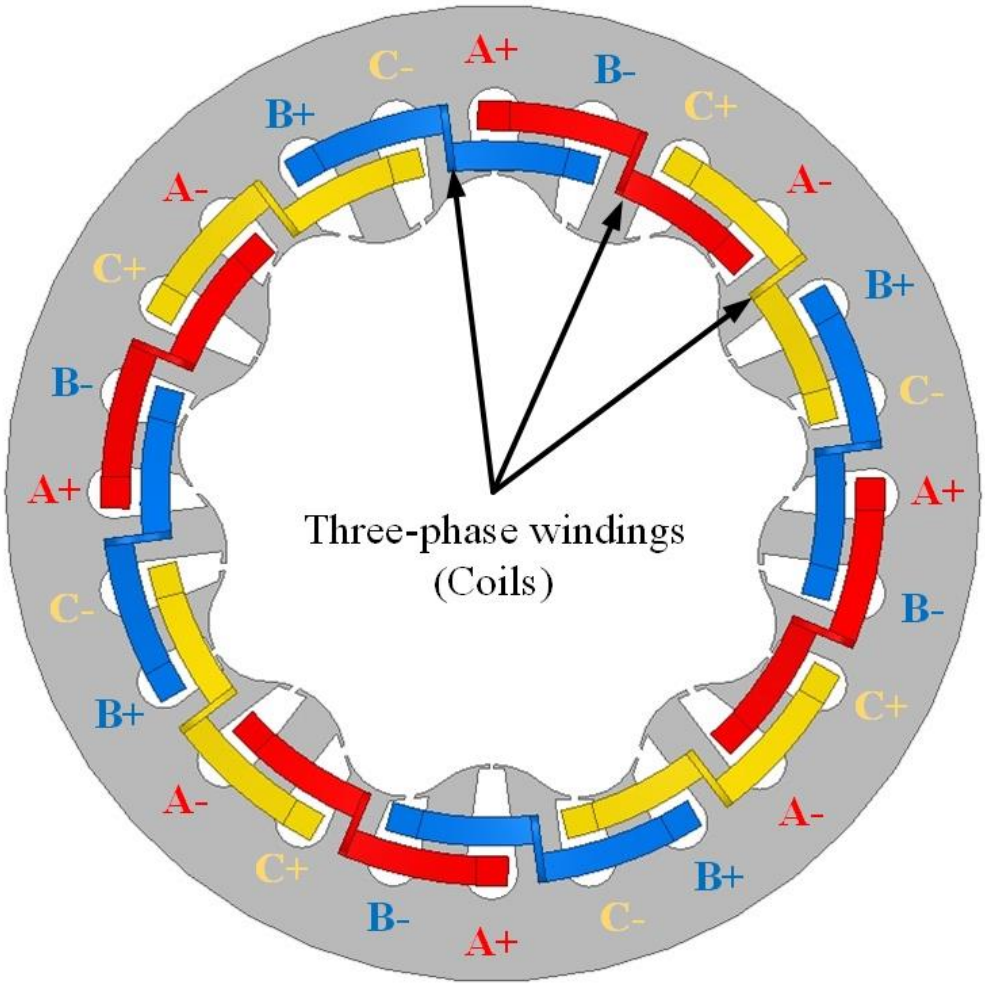

Figure 4.4 Coil distribution top view.

In the figure above, letters “A” “B” “C” indicate current phases. The symbol “+” implies the current forward direction at that position is flowing into the slot plane; while the symbol “-” indicates the current forward direction is flowing out of the slot plane. According to those symbols, connect adjacent “+” and “-” to form one coil terminal.

In addition, red coils correspond to phase A, blue coils indicate phase B and yellow coils represent phase C. Similar to motor stator coil distribution, these symmetrical three-phase coils would generate an eight poles rotating magnetic field which would attract magnets in the rotor and force the rotor to turn. Operating details would be discussed in next section.

4.2 Cycloid Electric Machine Operating Principle

In section 4.1, machine structure has been introduced, based on the structure, the operating principle will be discussed in this section. Chapter 3 explains that specifically distributed balanced AC current can generate a rotating magnetic field. Redraw the distributed current coils in Figure 4.2 and mark the poles generated by current field. Assume, the current is a balanced three phase sinusoidal wave with initial angle 0° and frequency 40Hz. At time 0, the poles distributed like Figure 4.2; as time moves on, three phases current amplitudes start to change, correspondingly, the current generated electromagnetic vector changes too. Due to three balanced phases regularly change, the resultant field vector would rotate in a

synchronous speed in physical space. The speed-current frequency relationship for the synchronous machine is the same as Equation (3.15).

When the stator generates magnetic field and form poles, distributed magnets in the rotor would be coupled with the field poles and follow them to rotate. Different from motor rotor, the cycloid rotor motion is a wobbling rotate, it rotates lobe by lobe and engages with stator internal surface. The ideal operating principle is shown in figure 4.5.

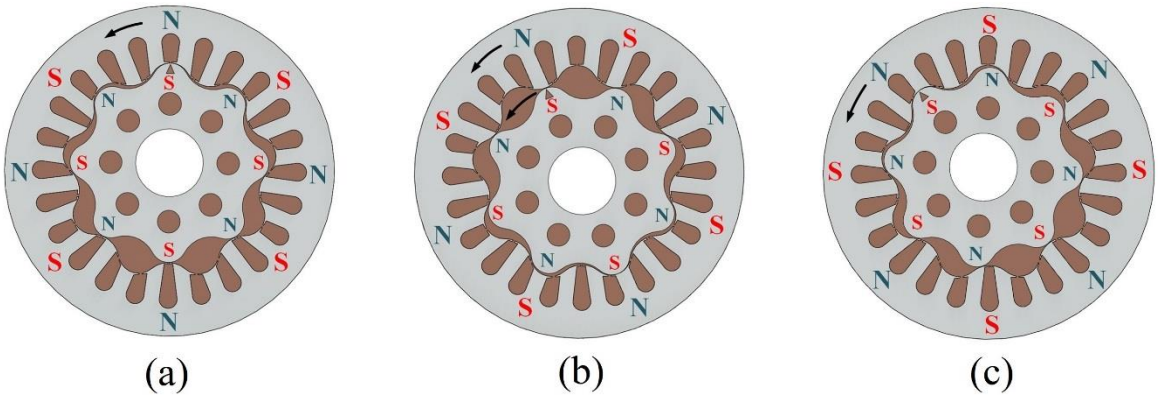

Figure 4.5 Ideal operating principle.

From the figure above, every lobe on the rotor is tracing the rotating magnetic poles due to the magnetic force. The magnetic pole sweeps every lobe on the stator, correspondingly, magnet lobes on rotor follow the poles and engage with stator lobes.

According to the wobbling rotation, the output holes on the rotor transfer torque to output plate pins, described in chapter 2, and finally deliver the torque to the output shaft.

4.3 Application Possibility

As the machine added electromagnetic torque, the multiple gear reduction stage would be eliminated. Therefore, the size and weight are reduced and the torque density is increased. This machine fits industries which require compact size and high torque density, such as the crane, medical devices, hybrid vehicle, and robotics. Moreover, this high torque density machine might replace present cycloid gear set if the output torque matches the requirements.

Chapter 5 : Finite Element Analysis (FEA) and Simulation

This chapter introduces the realization of proposed machine in software simulation. Through applying cycloid profile equations in SolidWorks, the proposed machine prototype is built, respectively, coils are drawn through ANSYS Maxwell. Due to the software limitation, the machine could not rotate as designed. Despite it, simulation results reveal the proposed machine's feasibility.

5.1 Build 3D Model in Software

SolidWorks is a computer aided-design solid modeler software, and use parametric settings to create the model. Usually, a model starts with a 2D sketch, by setting parameters such as the length of the line, tangent and perpendicular relationship between two geometries, users can easily build variable shapes. Moreover, SolidWorks provides a tool named Equation Driven Curve which facilitates users draw unique geometry like cycloid gear profile. After drawing a 2D sketch, the 3D model can be automatically built from feature settings.

Explained in chapter 2 that rotor profile can be drawn through Equations (2.1) (2.2) (2.3). Based on equation driven curve function in SolidWorks, the rotor profile is drawn as Figure 4.2 shows. In addition, to indicate output part, coupling holes are also drawn in the

rotor. The centered big hole is drawn for indicating the original input shaft. Correspondingly, the stator internal profile is derived from rollers shown in Figure 4.3. Slots between stator profile and outer edge are hollowed according to the format:

$$L_{\text{slot}} \leq 65\% \times W_{\text{stator}} \qquad \text{Equation 5.1}$$

where: L_{slot} is the length of the slot, and W_{stator} is the width of the stator at the slot's position.

With the help of the software, the virtual model can be established easily and accurately. However, geometry built in SolidWorks is unable to be modified in ANSYS, and coils drawn in SolidWorks are unable to be applied as excitation terminals in ANSYS. Due to this problem, the author draws coils in ANSYS Maxwell.

ANSYS is a computer-aided engineering software, it has many discipline products aiming to solve different industries problems. In this thesis, the author utilizes ANSYS Maxwell which is a Finite Element Analysis-based electromagnetic and electromechanical simulation software. Analysis function details would be introduced in the next section. In this section, the drawing function would be briefly introduced. As mentioned above, the author uses ANSYS Maxwell to draw coils by firstly import SolidWorks geometry in ANSYS workbench. Under the Cartesian coordinate system, directly use tools such as drawing arc, square, and lines at the specific position in slots. Then, by applying sweep

function, transform the two-dimensional graphic to a three-dimensional model. As the slots and coils are symmetrical, using duplicate and rotate function would simply finish the stator coils model. Completed geometry is shown in Figure 5.1.

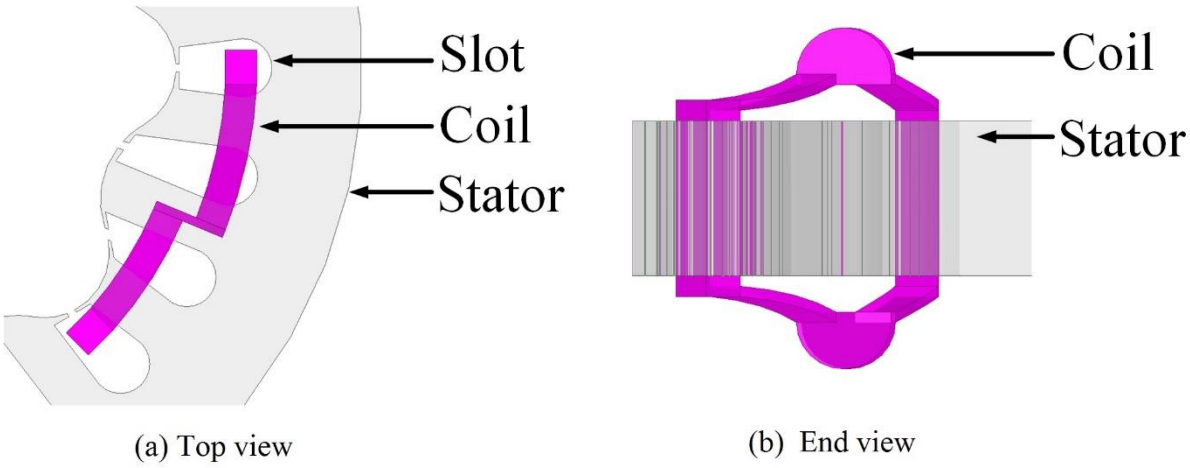

Figure 5.1 Coils in stator drawn in ANSYS Maxwell.

With this, the machine geometry is completed shown in Figure 4.1, the next step is to set up parameters and create simulation environment.

5.2 Finite Element Analysis and Simulation in ANSYS

In this chapter, the author briefly introduces the basic concept of finite element analysis (FEA), and present the model parameters applied in Maxwell geometry.

5.2.1 Finite Element Analysis (FEA) Introduction.

According to reference 9-11, finite element analysis (FEA) is a computational method applied for engineering analysis. Originally, FEA method is used for stress analysis for aircraft design. Now, it has been extensively applied in the analysis of fluid flow, heat transfer, electric and magnetic field and many other industrial designs. FEA can be generally understood as subdivide complexities into small units termed elements. After solving elements' properties, the next step is to assemble elements properties and use system equations to solve the whole system/structure problem [9-11]. FEA procedure diagram is shown in Figure 5.2 in terms of the book "Finite Element Analysis" written by Bhavikatti.

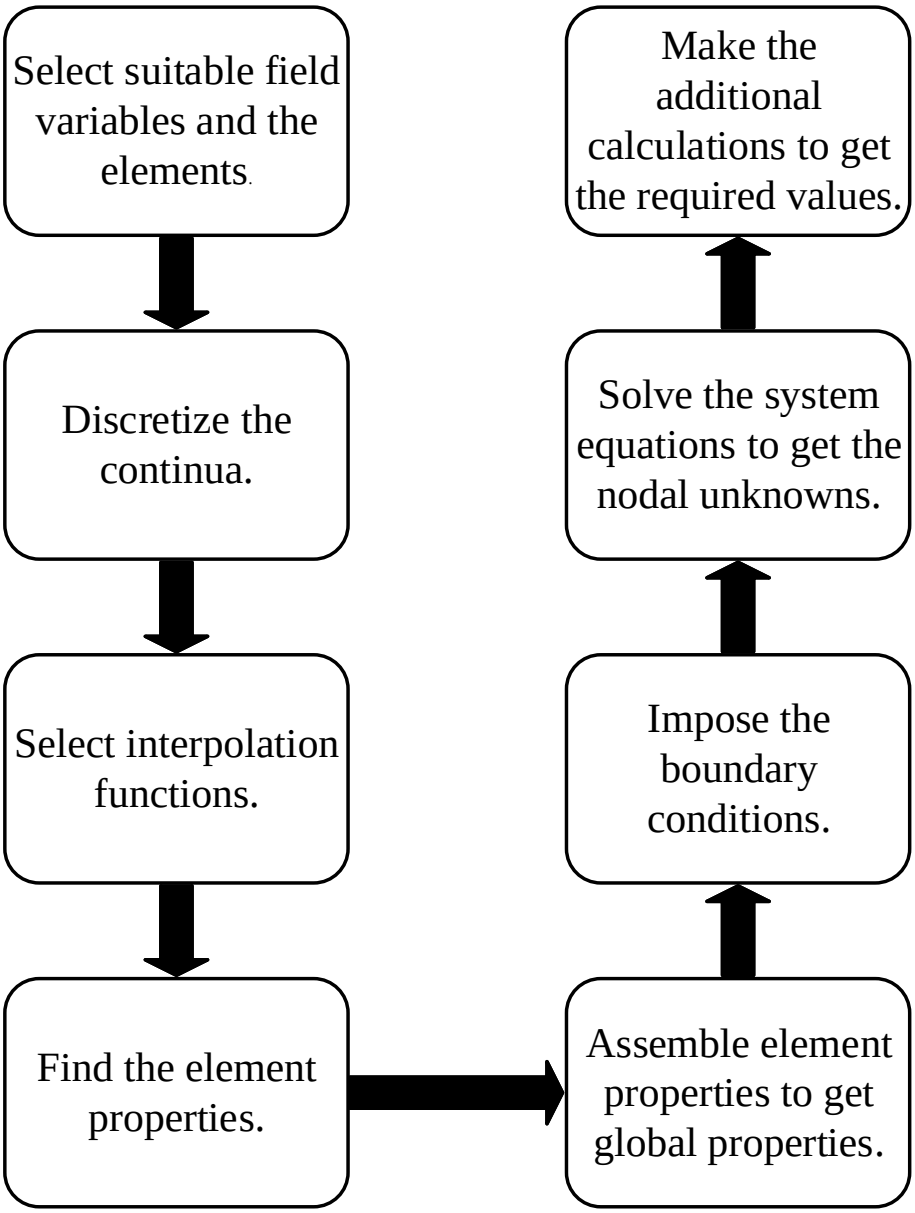

Figure 5.2 FEA analysis procedure.

Diagrams above includes eight steps leading to completed FEA. In ANSYS Maxwell, objects mesh settings correspond to subdivision step, region setting defines boundary condition.

5.2.2 Model Simulation

A 3D machine model has been built in ANSYS, in order to analyze output torque and flux distribution, simulation properties need to be set up in the process. Table 5.1 to 5.3 illustrate model dimensions, components' materials and excitation parameters (materials parameters come from reference [23]).

Table 5.1 Dimensions of proposed cycloid machine

Symbol	Geometrical meaning	Values
N	Stator lobes number.	9
L	Rotor lobes number	8
R	The length between stator lobe geometric center and stator geometric center.	46.2 mm
$\boldsymbol{R_r}$	Stator lobe radius	10.5 mm
E	Eccentricity, the length between rotor geometric center and stator geometric center.	3.2 mm
D	Stator outer diameters which defines the horizontal size of the machine.	130 mm
H	The thickness of the machine which defines the vertical size of the machine.	15 mm

Table 5.2 Model components materials

Components	Material
Stator	M19_29G (Electrical steel)
Cycloid Rotor	M19_29G (Electrical steel)
Permanent Magnets	N36Z_20 (Magnets)
Coils	Copper

The excitation parameters are summarized in table 5.2.2.

Table 5.3 Excitation current parameters.

Current parameters	Values
Magnitude $\boldsymbol{I_{MAX}}$	300A
Frequency	40 Hz
Number of conductors per winding	10

Before running analysis, the model needs to be meshed which corresponds to the first two steps of FEA method in Figure 5.2. Figure 5.3 shows the meshed model.

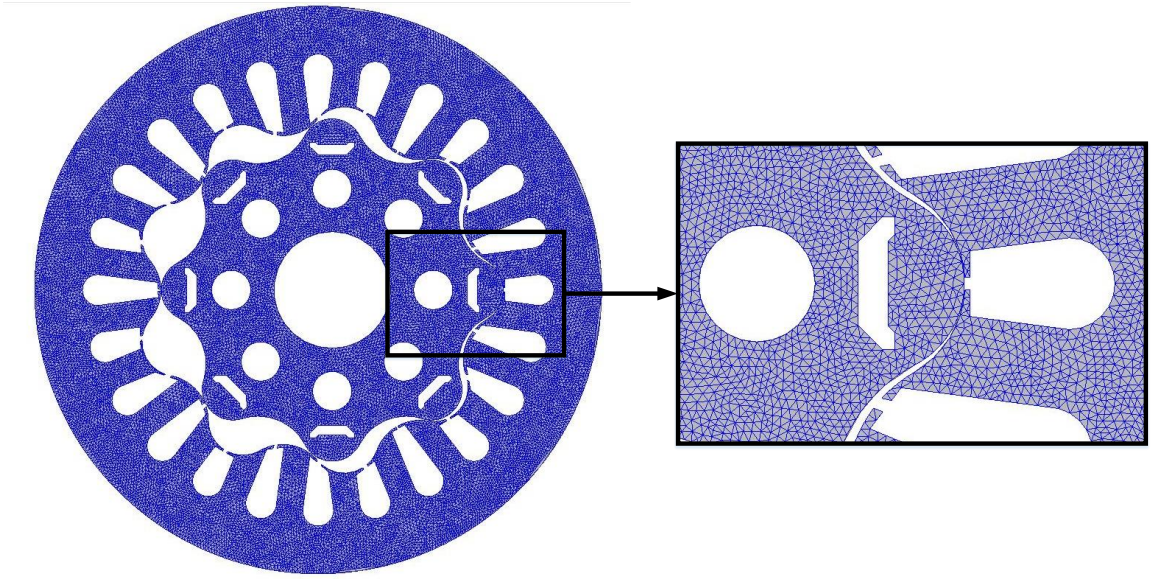

Figure 5.3 Model Meshing.

For the solution type, the author chooses Magnetic Transient Solver because the magnetic field varies with time. In terms of the operation set up limitation, ANSYS Maxwell does not provide cycloidal motion simulation. In motion settings, an isolated band object needs to be defined and it separates the rotor from stator without overlap [29]. This step is suitable for electric machines because between the rotor and the stator, there is a uniform air gap. A motion band object can be created in the air gap and enclose the rotor. However, the proposed machine rotates as tooth meshed, which means stator and rotor would contact with each other frequently, and the air gap is un-uniform and regularly varies

with time. Therefore, the band object would overlap with the stator, so that it is unable to set up cycloid motion.

Even so, the simulation results are still valid and rational. They would be analyzed in the next section.

5.3 Simulation Results and Analysis

In this section, simulation results are illustrated including output torque curve, flux distribution and same size PMSM output comparison. The torque output value may not accurate due to ANSYS limitation, but the comparison indicates that the output is reasonable and valid. However, the top concern with the machine is whether it would rotate as expected and how does it boost up the input torque. To clarify these two concerns, a analysis would be demonstrated at last.

5.3.1 Simulation Results.

Figure 5.4 (a) demonstrates the stationary rotor rotating magnetic field torque output. As the current frequency is 40 hertz, 25 milliseconds as one cycle, two cycles torque curve is performed. Due to ANSYS limitation, constant torque value cannot be obtained, to make an approximation, the curve's peak value is assumed as the maximum constant output torque. According to the results, a 130 mm diameter size cycloid electric machine with 10 conductors per winding may produce about 10 $N \cdot m$ torque output (see Figure 5.4 (a)).

Isolated result could not clarify the feasibility of the machine, therefore a same size same pole number PMSM is simulated as a reference model shown in Figure 5.4 (b). Note that the PMSM's rotor is stationary.

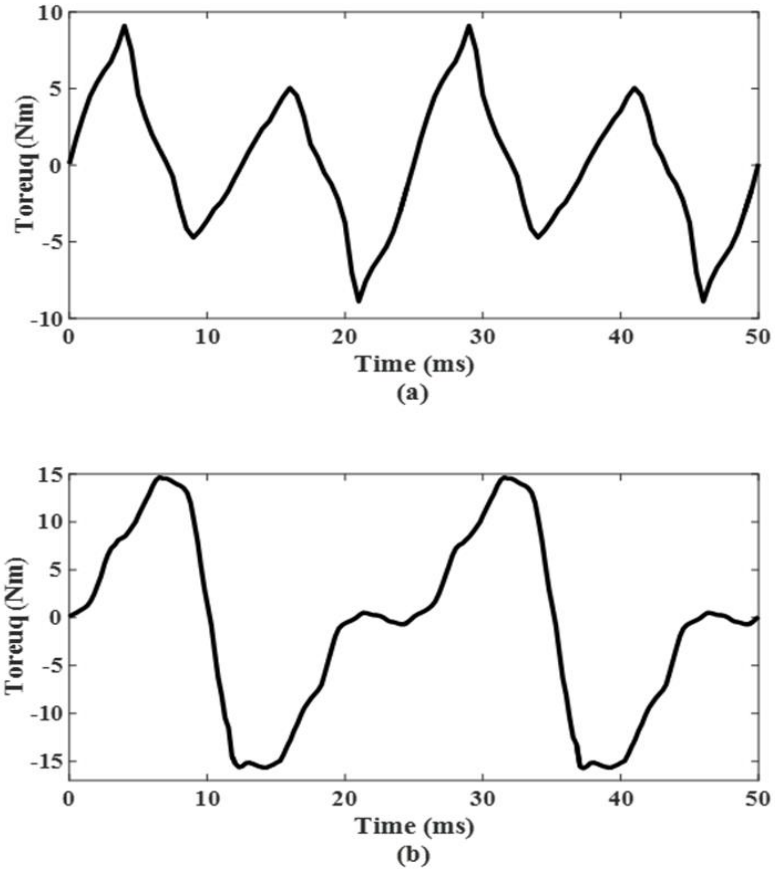

Figure 5.4 (a) Eight pole eight lobes cycloid electric machine output torque (b) eight poles permanent magnet synchronous machine (PMSM) output torque.

According to the figure above, the cycloid machine has more torque ripples in the same cycle, this is due to the asymmetrical distribution of rotor magnets relative to the stator. The PMSM output torque peak value is 5 N · m higher than that of the cycloid machine. To accurately obtain the output torque, a rotational rotor PMSM is simulated too. Figure 5.5 presents the average output torque of the PMSM with rotating rotor. It indicates that the average torque value is 13.99 N · m which is approximate to the torque peak value 15 N · m. Similarly, it can be derived that if the cycloid electric machine is able to rotate as expected, the average torque value may be approximate to the peak value 10 N · m. In order to achieve this goal, an analysis is presented in the next section.

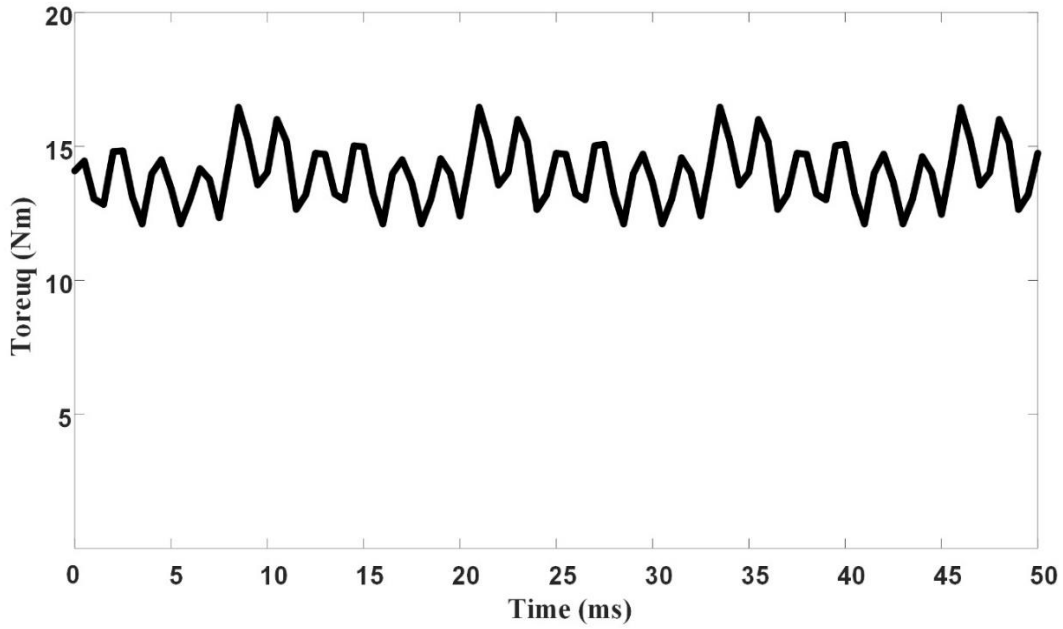

Figure 5.5 Output torque of reference PMSM.

Figure 5.6 illustrates the model flux distribution, it shows saturated areas where poles locate.

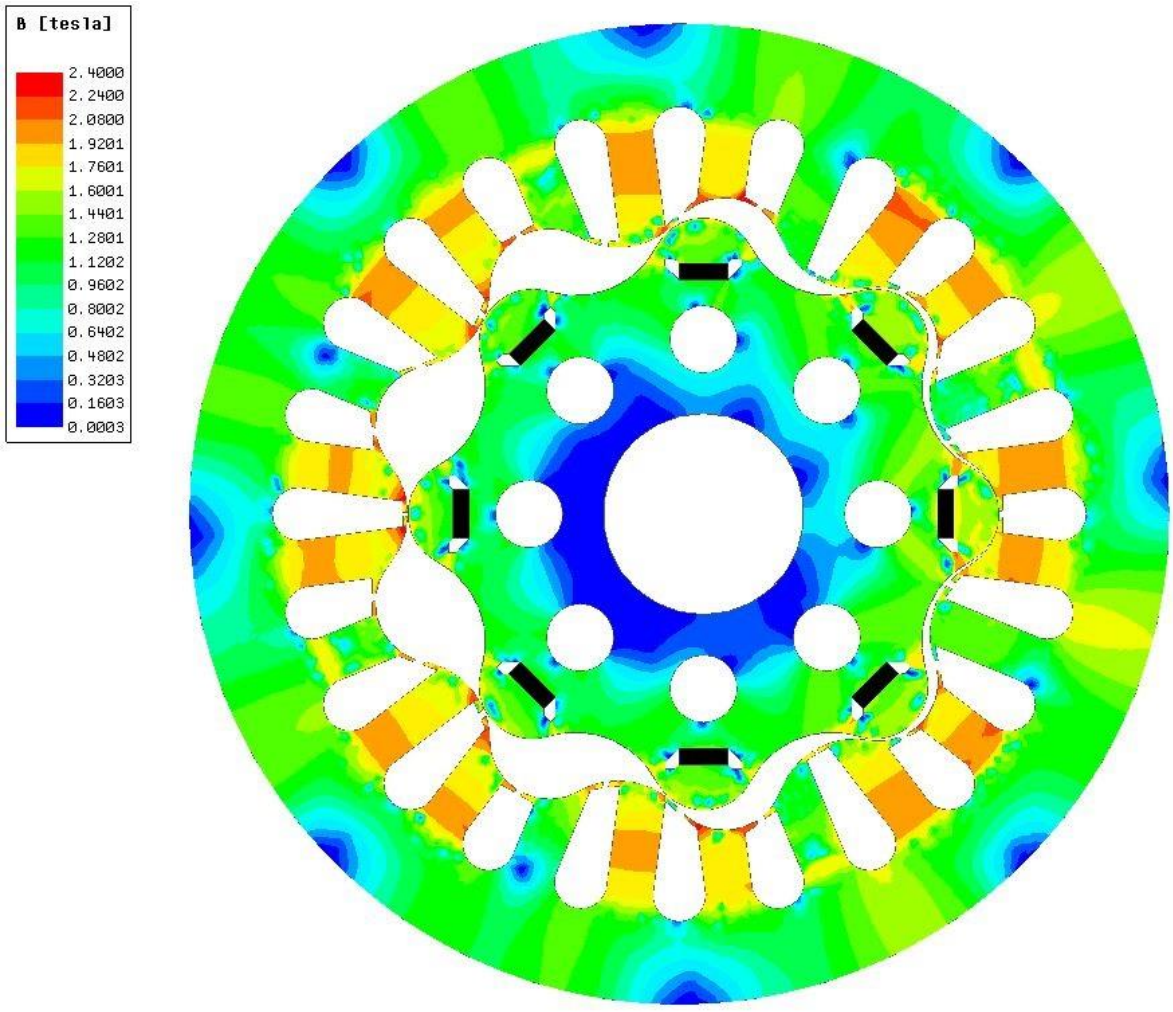

Figure 5.6 Eight pole eight lobes model flux distribution

In the figure, poles areas (orange areas) are highly saturated as expected. Those magnets areas which are close to poles are in high flux density, while those away from

saturated poles are in low flux density because the eccentric cycloid rotor. The eccentric rotor result to an asymmetrical magnets distribution, so does the magnetic force.

Chapter 6 : Conclusion and Future Work

6.1 Summary and Conclusions

In the robotic transmission system, generally, a low-torque electric machine is used to couple with a multi-stage gear reduction system to obtain the required torque density. However, the size and weight of the multi-stage reduction system and the output torque density cannot meet robotics communities' requirements. A novel cycloid electric machine is proposed to boost up the output torque density and replace the multi-stage gear box. In the proposal, a 40% size and weight reduction is expected. In this research, target size and weight could be easily obtained, but the required output torque density is remained to be discussed due to software limitation and simulation results analysis.

For the cycloid gear drive system, the eccentric cam pushes the cycloid gear lobe to engage with ring gear gap. When the cam turns one revolution, each lobe fills the corresponding gap one time, due to the gap number is one more than lobe number, the cycloid gear would move forward one gap displacement in the opposite direction of the eccentric cam. This delicate motion generates high gear reduction. Through investigation and discussion, it is found that the eccentric cam provides a linear force instead of rotational force to push the lobe against the gap. However, the proposed machine stator generates a rotational magnetic force which contributes to a slight increase in torque density and may

cause more chatter and wear. Therefore the linear force principle could be used to modify the proposed machine.

In conclusion, this research introduces basic concepts of cycloid gear drive and permanent magnet synchronous electric machine, builds up different type of 3D models for the proposed cycloid electric machine and conducts the model transient simulation. However the torque results do not reach the output torque requirement due to three reasons: first, no real sense of operating simulation is conducted, so it is uncertain that if this machine could work as expected and provide boosted output torque, besides, the existing result is smaller than the same size PMSM; second, the anticipative operating mode might be achieved, but the way in which the poles split the gear teeth weakens the transmission and would probably add noise and wear as the inner disk skips over the ring gaps (The expected operation is similar to electric machine eccentric operation, the contact between the rotor and stator would cause serious wear and tear); third, even though the machine operates as expected, it seems that this transmission does not take any advantage of the gear reduction because the armature winding generates the torque to the output side since there is no input side design. By deconstructing the machine's operation, it is found that the engagement between the rotor lobes and stator gaps is caused by a linear force. This motion character may produce a clue to reconstruct and improve the model. Possible solutions will be discussed in the next section.

6.2 Future Work and Discussion.

According to the gear ratio derivation of cycloid gear, increase rotor lobe number can obtain higher output torque as shown in Equation 6.1.

$$T_{\text{in}}(G_{\text{ratio}} + \text{k}) = T_{\text{out}} \quad (\text{k} \geq 1) \qquad \text{Equation 6.1}$$

Which is equal to:

$$T_{\text{in}}G_{\text{ratio}} + \text{k}T_{\text{in}} = T_{\text{out}} \qquad \text{Equation 6.2}$$

If the proposed machine is coupled with an input shaft, the output torque can be expressed as:

$$T_{\text{in}}G_{\text{ratio}} + T_{\text{magnetic}} = T_{\text{out}} \qquad \text{Equation 6.3}$$

In the Equation 6.3, the T_{magnetic} is the torque generated by the proposed machine. It reveals that the magnetic torque is independent of the gear ratio G_{ratio}. Compare Equation (6.2) with (6.3), only when $\text{k}T_{\text{in}} < T_{\text{magnetic}}$ will the existing structure be worthy to be applied. This approach constrains the input torque and further limits the output torque density. Moreover, by comparing the simulation results of 8-pole eight-lobe model (Figure 5.4 (a)) and 8-pole sixteen-lobe model (in the appendix B), the gear ratio absence is more evident. In terms of the cycloid gear operation (Equation 2.4), when the lobe number

increases from eight to sixteen, the sixteen-lobe model output torque value should be twice as that of the eight-lobe model. According to the results, the torque value increases from 9.5 N·m to 13 N·m which is not as two times as 9.5 N·m. This analysis denotes that in order to reach a certain value of torque, increasing the lobe number in cycloid drive system is more efficient and easier than adding armature windings in the proposed machine which consumes additional electric power to provide smaller torque and which complicates the overall structure. In mechanical aspect, those flux barrier chips and slots shown in Figure 4.3 weaken the machine's mechanical strength. Due to reasons above, the model structure might be unworthy to be applied.

Another possible project might solve the problem above, it changes the operating principle, and accordingly, modify the coil and magnets distribution. As introduced in section in 5.3.2 and 6.1, for cycloid gear drive, the eccentric cam provides a linear force to each lobe in turns as shown in Figure 6.1 (a). The designed magnetic field may replicate this operating principle and generates the torque on the input side. To realize this intention, the existing structure might be modified to a one pole machine. If the pole on the stator is able to attract rotor lobes in a linear way and push them to fill the gap, the magnetic torque may be transferred to the input side as shown in Figure 6.1 (b). Then, the cycloid gear reduction might be used. Therefore, the future work is to create a one pole machine that provides linear force on the lobe.

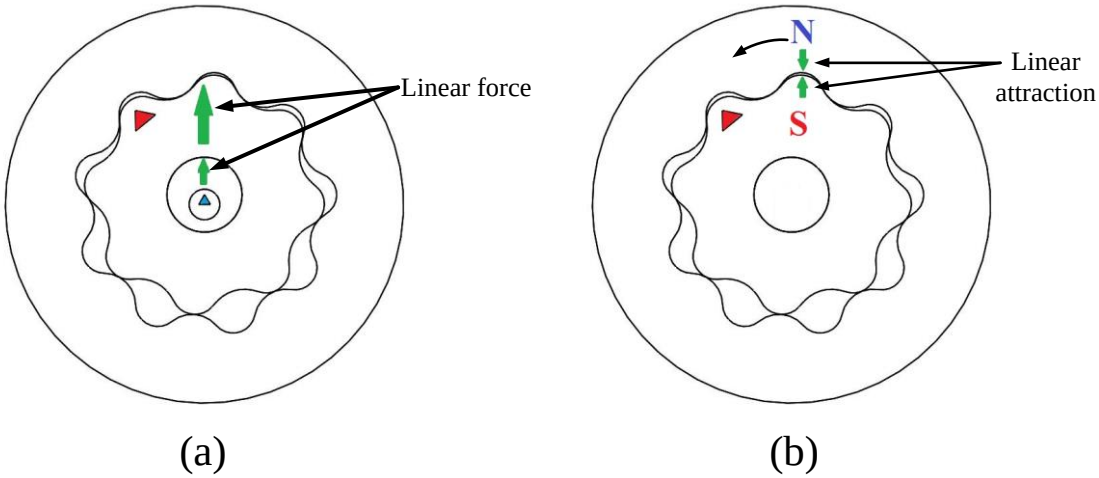

Figure 6.1 Linear force diagram. (a) Cycloidal gear drive linear force (b) proposed machine replicated linear force.

Bibliography

[1] J.-H. Shin and S.-M. Kwon, "On the lobe profile design in a cycloid reducer using instant velocity center," *Mechanism and Machine Theory*, vol. 41, no. 5, pp. 596–616, 2006.

[2] J. Nachimowicz and S. Rafałowski, "Modelling the Meshing of Cycloidal Gears," *Acta Mechanica et Automatica*, vol. 10, no. 2, Jan. 2016.

[3] Choi TH, Kim MS, Lee GS, Jung SY, Bae JH, Kim CC. Design of Rotor for Internal Gear Pump Using Cycloid and Circular-Arc Curves. ASME. J. Mech. Des. 2012;134(1):011005-011005-12. doi:10.1115/1.4004423.

[4] J. W. Sensinger and J. H. Lipsey, "Cycloid vs. harmonic drives for use in high ratio, single stage robotic transmissions," presented at the IEEE Conf. Robot. Autom., St. Paul, MN, USA, 2012.

[5] M. Neagoe, D. Diaconescu, C. Jaliu, L. Pascale, R. Saulescu, and S. Sisca, "On a new cycloidal planetary gear used to fit mechatronic systems of RES," *2008 11th International Conference on Optimization of Electrical and Electronic Equipment*, 2008.

[6] Vecchiato, D., Demenego, A., Argyris, J., and Litvin, F. L., 2001, "Geometry of a Cycloidal Pump," Comput. Methods Appl. Mech. Eng., 190, pp. 2309–2330.

[7] Kawahara S, Ohishi K, Miyazaki T, Yokokura Y (2013) Vibration suppression feedback control on angular transmission error of cycloid gear for industrial robot. In: Proc 2013 I.E. Int. Conf. Mechatron (ICM 2013), pp 859–864. Vicenza, Italy.

[8] Y.W. Hwang, C.F. Hsieh "Geometric design using hypotrochoid and nonundercutting conditions for an internal cycloidal gear"Journal of Mechanical Design, 129 (4) (2007), pp. 413–420

[9] Z. Ye, W. Zhang, Q. Huang, C. Chen "Simple explicit formulae for calculating limit dimensions to avoid undercutting in the rotor of a cycloid rotor pump" Mechanism and Machine Theory, 41 (2006), pp. 405–414

[10] Younis, "Building a Cycloidal Drive with SOLIDWORKS." [Online]. Available: http://www.bing.com/cr?IG=EFD8DAA1A91D43A4AC58FB0991AF7202&CID=1D74206646D068E21A362AEC47D669BE&rd=1&h=u3K2MkBFFHPG7cdojPYMN528MxgoBMJ5wpUEjUOpzsQ&v=1&r=http%3a%2f%2fblogs.solidworks.com%2fteacher%2fwp-content%2fuploads%2fsites%2f3%2fBuilding-a-Cycloidal-Drive-with-SOLIDWORKS.pdf&p=DevEx,5062.1. [Accessed: 22-May-2017].

[11] P. Shen, "Cycloidal equidistant curved gear transmission mechanism and its device," 08-May-1990. Patent number. 4922781

[12] Y.-W. Hwang and C.-F. Hsieh, "Determination of surface singularities of a cycloidal gear drive with inner meshing," *Mathematical and Computer Modelling*, vol. 45, no. 3-4, pp. 340–354, 2007.

[13] F. L. Litvin, A. Demenego, and D. Vecchiato, "Formation by branches of envelope to parametric families of surfaces and curves," *Computer Methods in Applied Mechanics and Engineering*, vol. 190, no. 35-36, pp. 4587–4608, 2001.

[14] Demenego, D. Vecchiato, F. L. Litvin, N. Nervegna, and S. Mancó, "Design and simulation of meshing of a cycloidal pump," Mechanism and Machine Theory, vol. 37, no.3,pp.311–332,2002.

[15] L. Lei, Y. Tao, and T. M. Guan, "Parametric Design of Cycloid Gear Based on SolidWorks," *Advanced Materials Research*, vol. 538-541, pp. 3106–3109, 2012.

[16] F. Joergensen, T. Andersen, and P. Rasmussen, "The cycloid permanent magnetic gear," *Conference Record of the 2006 IEEE Industry Applications Conference Forty-First IAS Annual Meeting*, 2006.

[17] R. Chicurel-Uziel, "Cycloidal Magnetic Gear Speed Reducer," *Modern Mechanical Engineering*, vol. 03, no. 04, pp. 147–151, 2013.

[18] Chen, B., Fang, T., Li, C. et al. Sci. China Ser. E-Technol. Sci. (2008) 51: 598. doi:10.1007/s11431-008-0055-3

[19] J. Zhang, T. Brekken, A. Jouanne, E. Cotilla-Sanchez, "High Torque Density Cycloid Electric Machines for Robotic Applications", A proposal to Grainger Center for Electric Machinery and Electromechanics. OSU July 7th 2016.

[20] Y. Song, Q. Liao, S. Wei, and L. Guo, "Research on pure rolling cycloid-like reducers used in industrial robot," *2014 IEEE International Conference on Information and Automation (ICIA)*, 2014.

[21] R. P. Shao, W. Wang, J. Li, and X. N. Huang, "Coupling Analysis on Dynamics and Tribology for Cycloid Transmission Used in Robot Joint," *Advanced Materials Research*, vol. 658, pp. 305–310, 2013.

[22] J. W. Sensinger, "Efficiency of High-Sensitivity Gear Trains, Such as Cycloid Drives," *Journal of Mechanical Design*, vol. 135, no. 7, p. 071006, 2013.

[23] thundergod88, "Maxwell3D User Manual Example of the 2004 Prius IPM Motor," Scribd.[Online].Available:https://www.scribd.com/doc/87741382/Maxwell 3D-User-Manual. [Accessed: 31-May-2017].

[24] A. E. Fitzgerald, C. Kingsley, and S. D. Umans, Electric machinery. New York: McGraw-Hill, 1983.

[25] J. K. Davidson, K. H. Hunt, and G. R. Pennock, "Robots and Screw Theory: Applications of Kinematics and Statics to Robotics," *Journal of Mechanical Design*, vol. 126, no. 4, p. 763, 2004.

[26] J. S. Dai and D. R. Kerr, “Geometric Analysis and Optimization of a Symmetrical Watt Six-Bar Mechanism,” *Proceedings of the Institution of Mechanical Engineers, Part C: Journal of Mechanical Engineering Science*, vol. 205, no. 4, pp. 275–280, Jan. 1991.

[27] J.E. Shigley, J.J. Uicker Jr., *Theory and Machines and Mechanisms*, McGraw-Hill, 1980.

[28] S. S. Bhavikatti, *Finite element analysis*. Place of publication not identified: New Age International Pvt, 2014.

[29] “ANSYS Maxwell V16 Training Manual - narod.ru.” [Online]. Available: http://www.bing.com/cr?IG=F3E47A9ACAAB4AE8A0F0D2BD915C303C&CID=01169F5345D56B9234F195D944D36A4A&rd=1&h=aBxLkGoi_cDz2xZ54NYqiwF-_s9q5FtMQjhc9XJKJrg&v=1&r=http%3a%2f%2fansoft-maxwell.narod.ru%2fen%2fMaxwell_v16_L05_Transient_Solvers.pdf&p=DevEx,5055.1. [Accessed: 22-May-2017].

Appendices

Appendix A Six Pole Six Lobes Rotor Model Simulation Results.

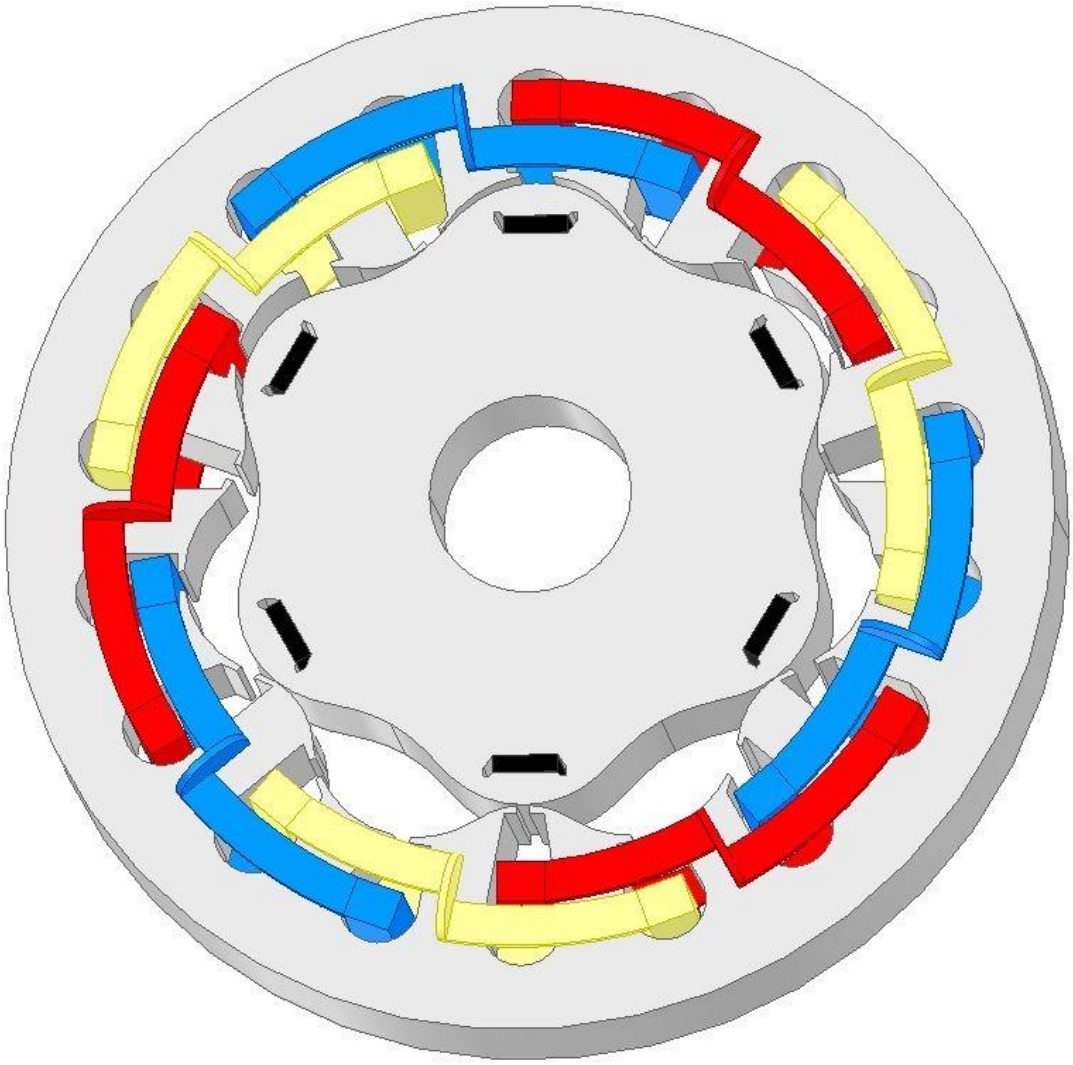

Figure_Apx 1 Six pole six lobes model.

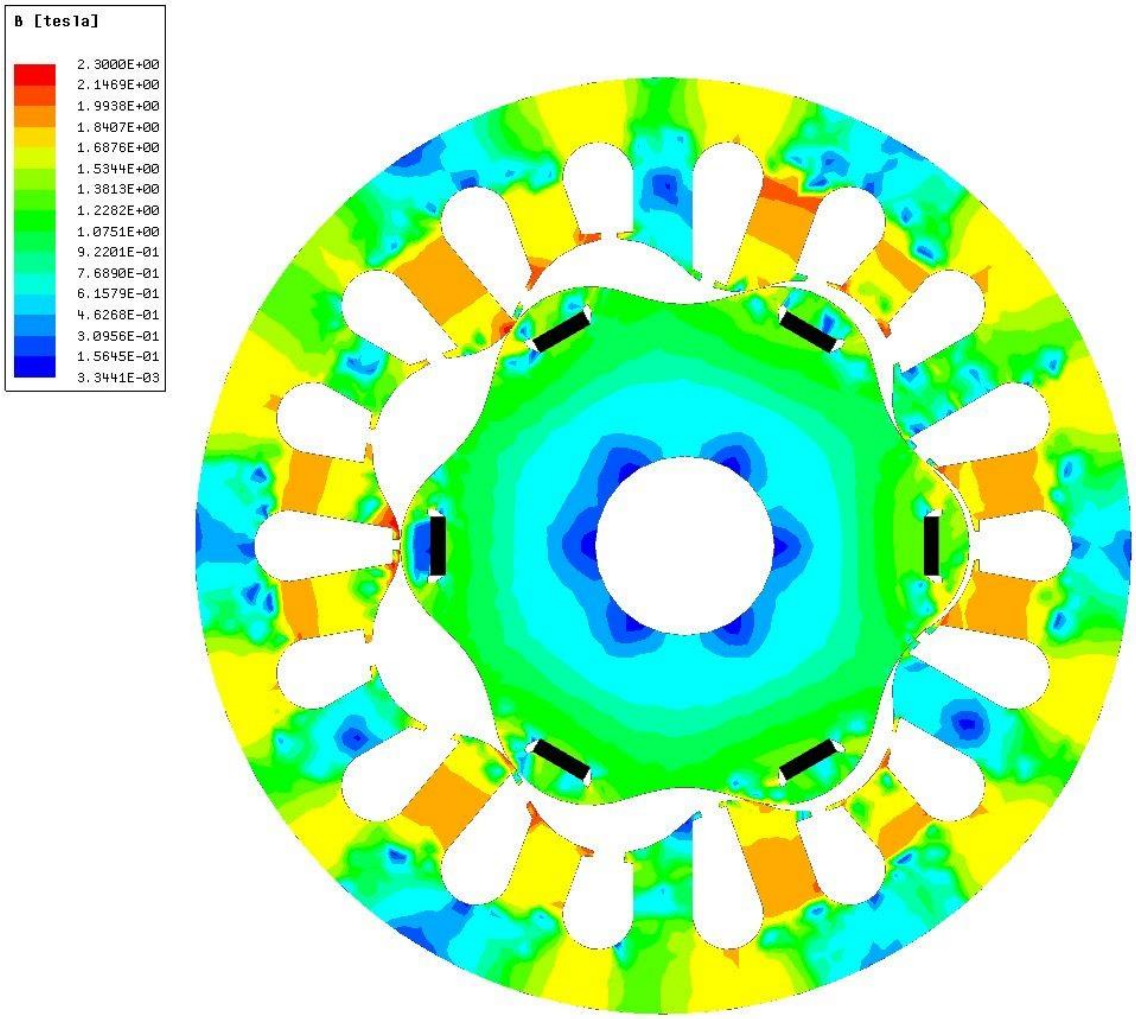

Figure_Apx 2 Six pole six lobes model flux distribution.

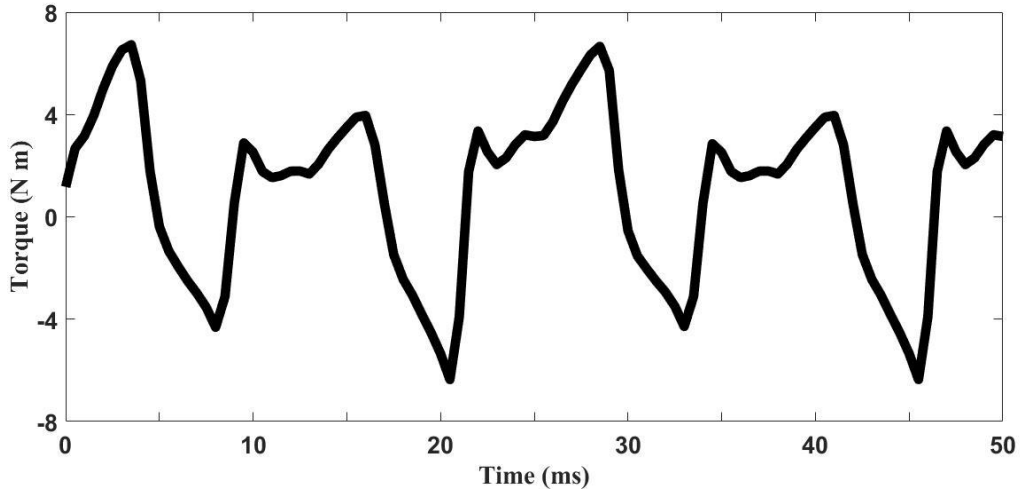

Figure_Apx 3 Six pole six lobes six poles model output torque.

Appendix B Eight Pole Sixteen Lobes Rotor Model Simulation Results.

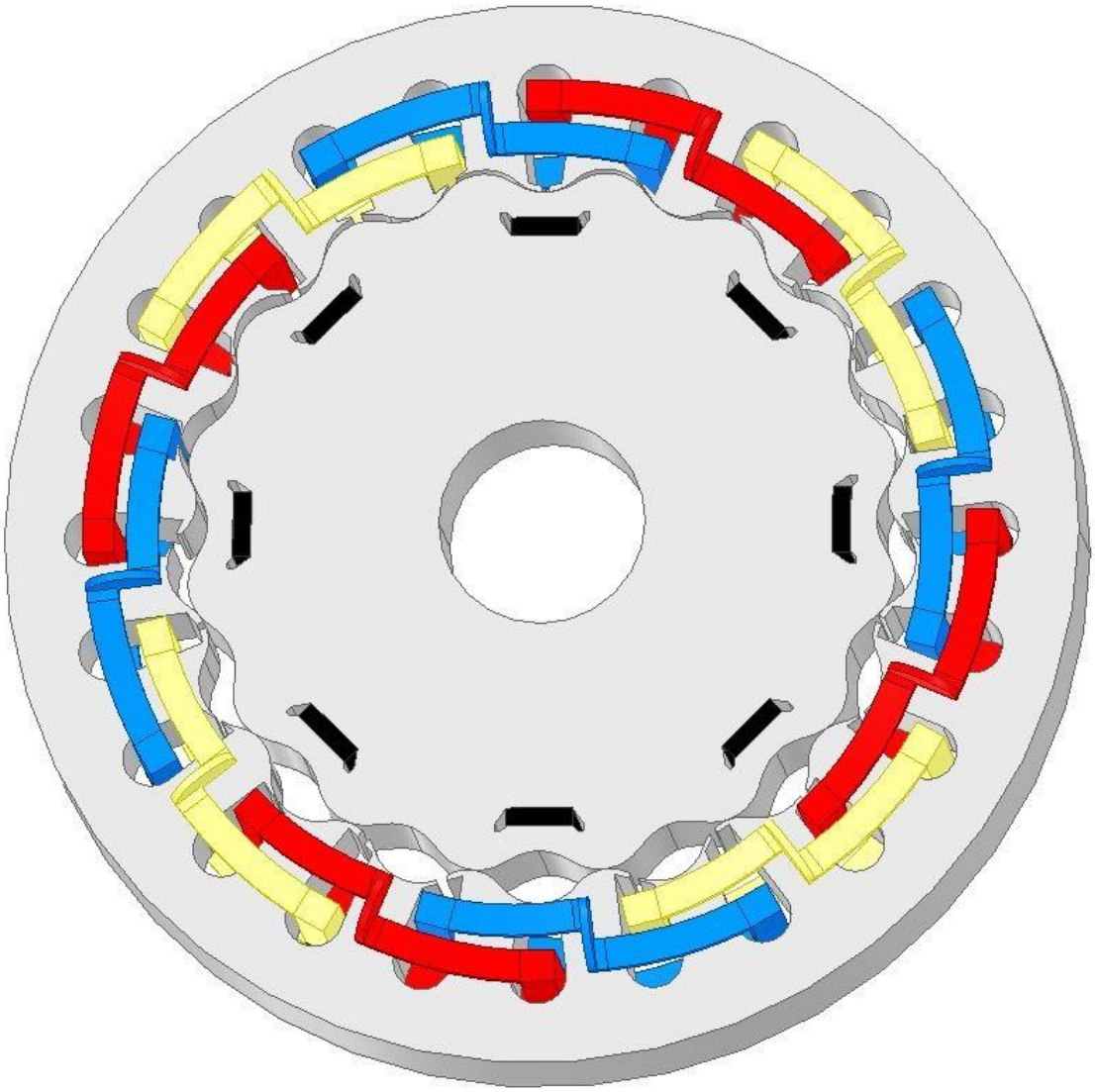

Figure_Apx 4 Eight pole sixteen lobes model.

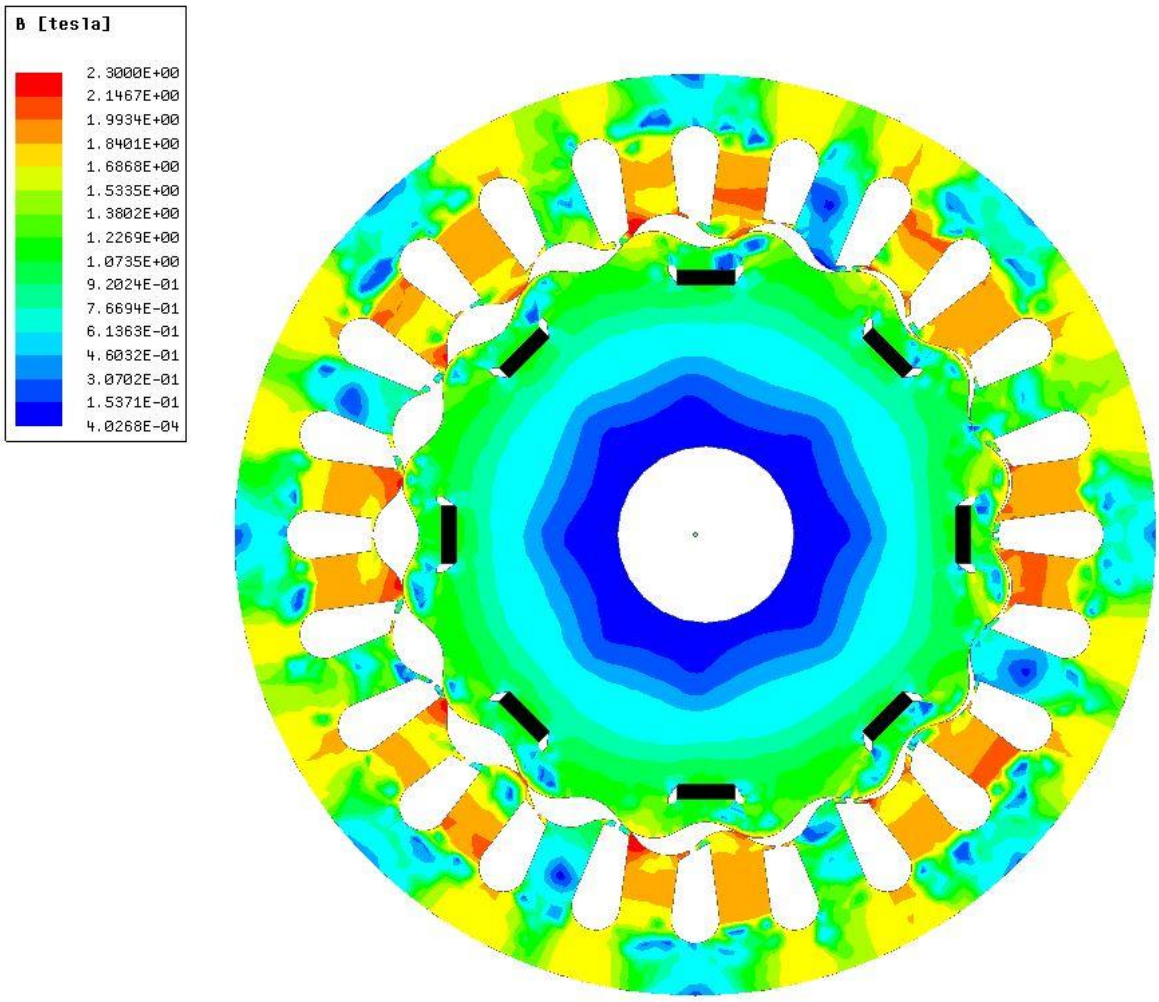

Figure_Apx 5 Eight pole sixteen lobes model flux distribution.

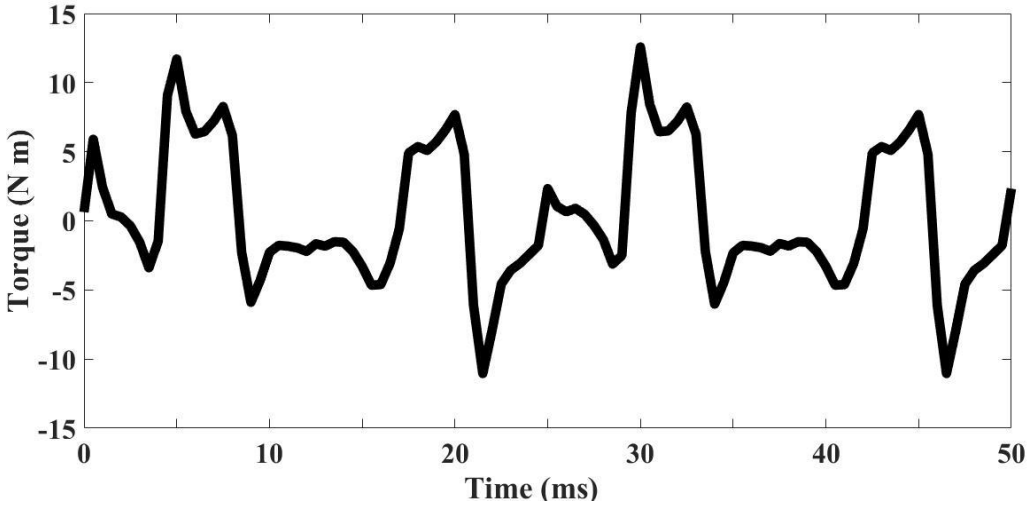

Figure_Apx 6 Eight pole sixteen lobes eight poles model output torque.